ISSN 2463-6029 (Print)

ISSN 2350-3432 (Online)

Recent and Historical Sedimentation and Sediment Characteristics of Ōhiwa Harbour, New Zealand

ERI Report Number 156

By Andrew D. La Croix

Client report prepared for Bay of Plenty Regional Council

8 March 2022

Email: alacroix@waikato.ac.nz

Environmental Research Institute
Division of Health, Engineering, Computing & Science
University of Waikato, Private Bag 3105
Hamilton 3240, New Zealand

THE UNIVERSITY OF WAIKATO
Te Whare Wānanga o Waikato

Environmental Research Institute
Te Pūtahi Rangahau Taiao
THE UNIVERSITY OF WAIKATO

Cite report as:
La Croix AD. 2022. Recent and Historical Sedimentation and Sediment Characteristics in Ōhiwa Harbour, New Zealand. *Environmental Research Institute Report No. 156*. Client report prepared for Bay of Plenty Regional Council. Environmental Research Institute, Division of Health, Engineering, Computing & Science, The University of Waikato, Hamilton. 47 pp. ISSN 2463-6029 (Print), ISSN 2350-3432 (Online).

Reviewed by:

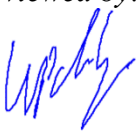

Dr. Willem De Lange
University of Waikato

Approved for release by

Dr. Charles Lee
University of Waikato

Executive Summary

The Bay of Plenty Regional Council is seeking to understand historical and recent sedimentation in Ōhiwa Harbour, a barrier-enclosed lagoon, to help establish sediment accumulation rates and water quality limits in accordance with the Resource Management Act (1991) and the NZ Freshwater Policy Statement. To provide sedimentation data that is independent of sediment plate data already being collected by the Council, and to supplement other historical data, a series of nine vibracores, nine box cores, and 73 surface sediment samples were collected from across Ōhiwa Harbour.

Three key vibracores were analyzed for their radionuclide activity (^{210}Pb and ^{226}Ra) in an attempt to determine their sediment accumulation rates. However, no rate could be established due to very low and irregular radionuclide activity through the cores. It is probable that the method did not work due to the combined effects of hydrodynamic mixing and bioturbation.

Sedimentological analysis was undertaken on all nine vibracores and box cores, which indicated that the intertidal sediments consist of five distinctive depositional units: clast supported calci-gravel, ripple to cross bedded sand, bioturbated sand, laminated to rippled silt, and bioturbated silt. Recognition and interpretation of these units will be useful for future workers interested in reconstructing the evolution of sedimentation within the harbour.

Grain size of core sediment and surficial sediment around the harbour was compared to historical surface sediment maps. They show clearly that Ōhiwa Harbour is becoming muddier through time, although in a non-linear and complex way with some parts of the harbour getting sandier. The perimeter of the harbour and the upper harbour are the main areas affected by a fining grain size trend.

Loss-on-ignition (LOI) of sediment indicates that organic carbon is more concentrated in fine-grained sediment than coarser sediment across the harbour. No clear stratigraphic pattern of LOI could be established. However, surface sediments display larger LOI along the perimeter of the harbour where the proportion of mud is greater.

Three recommendations are put forth based on the results of this study, as well as gaps in knowledge discovered during data collection and analysis. The first is that determining longer-term (decades–millennia) sediment accumulation rates may be achievable by carbon-dating the abundant shell material contained within cores. The second is that calculation of sediment compaction under its own weight (‘autocompaction’) may help determine the causes of sedimentation and erosion in the harbour. The third and final recommendation is for repeat surface sediment surveys to be undertaken regularly, at intervals no greater than every five years. These insights will together yield a more complete picture of past, present, and future sedimentation and its effects in Ōhiwa Harbour.

Table of Contents

List of Tables

List of Figures

1. Introduction

The deterioration of estuaries due to contamination by sediment, nutrients, and other pollutants flowing from river catchments to the land-sea interface is a significant global problem (Lotze et al., 2006). Land use changes, a growing population, and anthropogenic-linked climate change are altering river discharge patterns, increasing soil erosion, and affecting eutrophication with negative consequences for marine ecosystems and the sustainability of the ocean as a breadbasket (Kennish, 2001; Nixon, 2012; Schiel and Howard-Williams, 2016). One of the major variables connecting human impact on land with the coastal oceans is the sediment flux through rivers and estuaries, with increases in sedimentation rates acting as a key environmental stressor (MacDiarmid et al., 2012). In New Zealand sediment yield from rivers to the ocean is large (>1000 t km-2 a-1; Hicks et al., 2011; Milliman, 1990), controlled by a young erodible geology, a steep mountainous landscape, and generally high rainfall (Basher, 2013; Soons and Selby, 1992). Notwithstanding the natural controls on sediment yield, studies have shown that New Zealand estuaries have been infilled with river-derived sediment at increasing rates since the arrival of Polynesians (ca. 1300 A.D.) and even more profoundly in the post-European era (Hunt, 2019; Nichol et al., 2013; Sheffieldt et al., 1995). Such increased sedimentation has had marked negative consequences for estuarine and coastal biodiversity and productivity (Thrush et al., 2004), which has disproportionately affected Māori communities who live on the coast (e.g., Paul-Burke et al., 2018).

Sediment core studies of estuaries on New Zealand's North Island have clearly demonstrated that sediment accumulation rates (SAR) during the pre-Polynesian era ranged from 0.2-2 mm yr^{-1} (Harpur, 2016; Hume and Dahm, 1992; Hunt, 2019; McGlone, 1989; Naish, 1990; Swales and Hume, 1995; Swales et al., 2005). By contrast, in the last century, the rates have increased markedly to between 2-200 mm yr^{-1} (Bentley et al., 2014; Huirama et al., 2021; Hume and Dahm, 1992; Hunt, 2019; Swales and Hume, 1995). These studies, however, have been challenged by the limitations associated with age-dating sediments using the ^{14}C or ^{210}Pb methods (Appleby, 1998; Barsanti et al., 2020; Petchey, 2009), and therefore it is unclear how meaningful reported estimates of "average" SAR over these time spans are given the inherently incomplete nature of the stratigraphic record (Paola et al., 2018; Straub et al., 2020). Nonetheless, the distinct increase in the range of SAR through time has also brought with it shifts in the texture of substrates (i.e., sand versus mud), as well as spatially heterogeneous changes in the balance between erosion and deposition (e.g., Anderson et al., 2004; Swales et al., 2007).

In response to the sedimentation problem, New Zealand is building policy around water quality and sedimentation limits that are required by the Resource Management Act (1991) and the NZ Freshwater Policy Statement (which includes estuaries) (M.F.E., 2020). Establishing these limits necessitates an estimation of "natural" and "contemporary" SAR, the former which is a historical undistributed baseline of sedimentation that pre-dates human occupation of New Zealand (i.e., for native forest catchments). The current recommendation for acceptable contemporary SAR is 2 mm yr^{-1} above the baseline, a rate considered necessary to avoid catastrophic damage to the estuarine macrobenthos community (Townsend and Lohrer, 2015).

As with most estuaries in New Zealand, sedimentation is a significant environmental issue for Ōhiwa Harbour (Senior et al., 2009). Increased sediment loads deliver excess nutrients and faecal material that reduced water quality, adversely affecting key shellfish, fish, and bird populations (Park, 2005). Furthermore, poor water quality is deleterious for aquaculture and

recreational use of the harbour. In order to mitigate this problem the Bay of Plenty Regional Council (BoPRC) installed sediment plates to measure SAR in 2010, but is seeking independent data to verify these measurements and to support development of water quality and sedimentation limits. This report presents the findings of a study commissioned by BoPRC which sought to determine long-term SAR across the harbour using ^{210}Pb age-dating of sediments from core. As a secondary objective, the report describes the sediment characteristics and distribution, as well as the stratigraphic stacking patterns within Ōhiwa Harbour.

2. Study Area

Ōhiwa Harbour is located on the east coast of the North Island of New Zealand, southeast of Whakatāne (Fig. 1). The harbour is an estuarine lagoon, sheltered from the Bay of Plenty (Pacific Ocean) by the Ōhiwa and Ōhope sand spits, which are dissected by a tidal inlet that is ca. 600 m wide at high tide. The harbour has a perimeter of 48 km and spans an area of 24 km^2 , with up to 70% of the harbour exposed at low tide (Gibb, 1977; Paul, 1966; Richmond et al., 1984). Broad tidal flats with slopes of less than 3º rim the harbour, generally having topographic relief of less than 1 m (Richmond et al., 1984). The upper tidal flats (ca. 40% of intertidal area) are covered with *Salacornia, Juncus,* and *Leptocarpus* salt marsh and are dissencted by streams flowing into the harbour. Up to 25% of the upper tidal flats are colonized by dense *Avicennia resinifera* mangrove forests. The lower tidal flats (ca. 60% of intertidal area) are cross cut by meandering tidal channels and small tidal creeks (Richmond et al., 1984). Mean depth in Ōhiwa Harbour is 2 m, with a maximum depth is 14 m, and a volume at high tide of 49.4 x 10^6 m^3 (Freestone, 1976; Richmond et al., 1984).

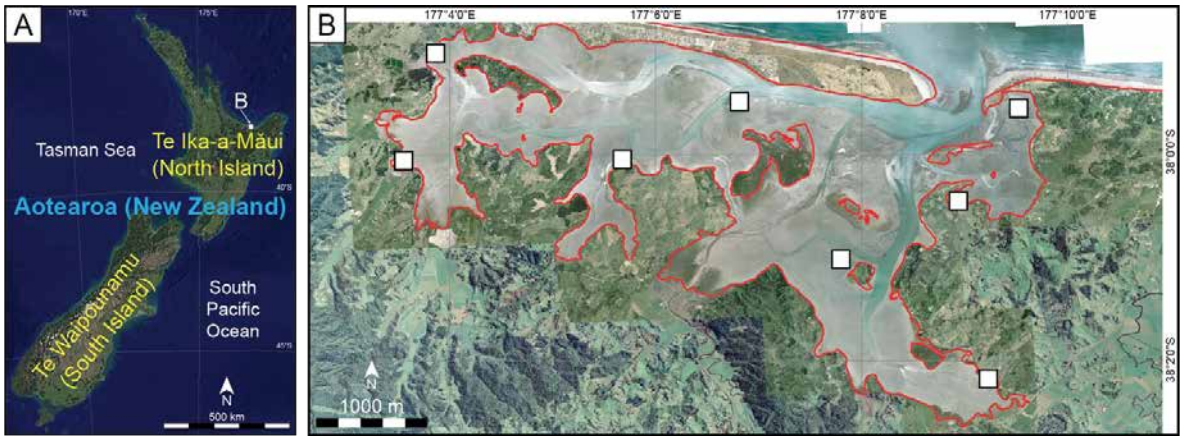

Figure 1: A) Location of Ōhiwa Harbour in Aotearoa New Zealand. B) Location of the nine cores and associated surface sediment samples that were analyzed as part of this study.

Tides in Ōhiwa Harbour are semidiurnal with a neap-spring range of 1.6-2.5 m. Water flow is overwelmingly dominated by tidal currents, with velocities up to 125 cm s^{-1} through the mouth of the inlet (Freestone, 1976; Richmond et al., 1984). Freshwater discharge into the harbour is very small – ca. 1.2 m^3 s^{-1} (Freestone, 1976) – as is land-derived sediment supply. Most of the water and sediment comes from the Nukuhou River, with a smaller proportion from the Awaraptuna, Pukehoko, Waiotane, Wainui, Te Awawairoa, Kutarere, and Te Kaha streams. The rest of the sediment in the harbour is carried into the mouth of Ōhiwa Harbour by longshore currents from the Whakatāne River (Healy, 1978). Tidal flushing of the lagoon is rapid with a water residence time of only 1-2 tidal cycles (Richmond et al., 1984). Wind-induced waves along the margins of the harbour can reach heights up to 0.5 m, with

predominantly northwesterly, northerly, and southerly directions of propogation (Richmond et al., 1984).

The mountainous catchment of Ōhiwa Harbour has an area of 172 km^2 with a maximum elevation of 371 m above sea level. About 18% of the land is covered by exotic plantation, 20% is indigenous forest, 14% is indigenous scrub, 44% is pasture, 1% is urbanized area, with the remaining few percent comprising exotic scrub, horticultural land, saltmarsh and wetlands, and water bodies (MacKenzie, 2013). The harbour is situated on the eastern end of the Whakatāne Graben, which is subsiding at a rate of 1-2 mm yr^{-1} (Beanland and Berryman, 1992), and lies adjacent to the uplifting Raukumara Ranges, between the Ōhope and Waikaremoana Faults (Beanland and Berryman, 1992; Hayward et al., 2004). The hills surrounding Ōhiwa Harbour comprise mid-Pleistocene sedimentary strata of the Ōhope Formation, which rests unconformably atop Mesozoic greywacke (Healy, 1967). These pass upwards into late-Pleistocene sedimentary strata and tephras of the Waiotahi Gravels and Ōhiwa Harbour Subgroup, respectively (Manning, 1996). The inner harbour of Ōhiwa overlies Pleistocene sedimentary rocks and tuffs of the Huka Group, but islands within the harbour may also consist of consolidated modern sediments (i.e., Tern and Motuotu islands) (Richmond et al., 1984). The mineralogy of sediment diverges somewhat between the upper harbour and lower harbour. In the upper harbour sediments are dominated by volcanic glass, pumice fragments, and feldspar, with subordinate amounts of quartz and biogenic calcite. By contrast the lower harbour is enriched in quartz and feldspar, with relatively less volcanic grains (Richmond et al., 1984).

During the last glacial maximum (21,000 ka) sea level was 134 m lower than present (Lambeck et al., 2014), and in the area around Ōhiwa Harbour rivers flowed northwards to a coastline situated offshore of its present position. Sea level rose gradually to flood the continental shelf and construct most of New Zealand's estuaries from 12,000 to 7,000 ka (e.g., Hemmingsen, 2001; Kirk and Lauder, 2000). From 7,000 ka to present sea level has varied over a much narrower range (i.e., +/- ca. 3 m; King et al., 2020). The last 100 years has seen a dramatic increase in the rate of rise in relative sea level to 2.8 mm/yr (King et al., 2020). A number of workers have studied the formation and evolution of Ōhiwa Harbour, especially in relation to changes in the barrier sand spits (Gibb, 1977; Hayward et al., 2004; Murdoch, 2005; Richmond et al., 1984; Robinson, 2012; Smith, 1976). The most recent interpretation, based partly on the presence of key ash beds, posits that the Ōhope and Ōhiwa spits were built following the Holocene sea level stillstand (7410-5175 yr BP; Julian, 2006), and that the harbour realized its most recent configuration somewhere around 575 yr BP (Murdoch, 2005).

3. Methods

To assess SAR, sedimentary history, and sediment characteristics of Ōhiwa Harbour, vibracores, box cores, and surface sediment samples were collected from nine stations across the lagoon (Fig. 1B; Table 1). The stations were situated in close proximity to sediment plates installed by the BoPRC. Cores were collected at intertidal positions in an effort to intersect as much of the historical subtidal sediments as possible. A box core was collected within 10 m of each vibracore to visualize the details of the sediment at depths up to 30 cm. Finally, surface sediment samples were collected from the upper 0-2 cm, arranged in a grid around each coring site. In total, nine vibracores, nine box cores, and 73 surface sediment samples were collected in April 2021.

Table 1: Vibracore locations within Ōhiwa Harbour.

Core	Latitude	Longitude	Length (m)
A	37.984260° S	177.0643117° E	2.37
B	37.991468° S	177.1123529° E	2.29
C	38.007395° S	177.1489488° E	2.32
D	38.001247° S	177.0591144° E	3.18
E	38.000090° S	177.0953057° E	2.09
F	38.016557° S	177.1309827° E	2.79
G	37.991013° S	177.1600080° E	3.38
H	38.036095° S	177.1540209° E	2.42

After vibracores were pulled from the ground, the ends of their 76.2 mm aluminum tubes were sealed watertight for transport back to the University of Waikato. In the laboratory, vibracores were split in half, wrapped in plastic, and the duplicates stored in a refrigerator at 6º C. Cores were then photographed in natural light and x-radiographed using a Cubex 50 portable x-ray machine operating at 90 kV and 1.30 mAs. The x-rays were measured on a Canon MXD DR9000 flat panel detector. The vibracores were logged for their grain size and lithology, bioturbation intensity (using the Bioturbation Index; Taylor and Goldring, 1993), physical sedimentary structures, and shells or accessories. The cores were then sampled every 2 cm down the core for the first 10 cm (i.e., 0-1 cm to 10-11 cm) and then every 5 cm to their base. Box cores were processed in the same manner as vibracores.

After sampling from the vibracores the sediment was immediately placed in whirl-pak bags to seal in moisture and stored in a refrigerator at 6º C. The samples were shipped to Flett Research Limited in Winnipeg, Canada, for determination of ^{210}Pb activity by measuring the granddaughter, ^{210}Po, using a modification of the alpha spectrometry procedures described in Eakins and Morrison (1978). The laboratory also determined the activity of ^{226}Ra by measuring ^{222}Rn emination, using a proceedure modified from Mathieu et al. (1988). Further details about the sample processing and detection methods can be found in Appendix A.

A second set of the vibracore samples, along with surface sediment samples, was dried at 60º C for 24 hours. Alloquots of a few grams of sediment were treated with 30% H_2O_2 to remove organics, 10% HCl to remove carbonates, and a 5% Na-Hexametaphosphate solution was added to deflocculate clays. Treated samples were seived through a 2 mm mesh and then run through a Malvern Mastersizer to determine the grain size distribution. Statistical treatment of grain size data used GRADISTAT (Blott and Pye, 2001). Another set of sediment sample alloquots were dried a second time at 105º C for 24 hours, weighed, heated to 430º C for 4 hours, and then weighed again in a modified version of the loss-on-ignition (LOI) method of Wood (2015). The final difference in mass was considered to be a proxy for total organic carbon. Grain size and LOI data were plotted next to lithologs and also used to construct station specific distribution maps using Esri ArcGIS. Grain size profiles and maps used the Folk and Ward (1957) mean, as well as the percentage of mud (<62.5 µm).

4. Results and Interpretation

4.1 Radionuclide Analysis

4.1.1 Core D Results

A regular ^{210}Pb profile exhibits an exponential decrease in total ^{210}Pb activity as a function of depth. Core D shows an irregular ^{210}Pb profile. The 2^{210}Pb activities vary between 0.75-1.26 DPM/g in the upper 23 cm (extrapolated depth) of the core, then decrease to 0.32 DPM/g in section 35-36 cm (extrapolated depth 30.5-43 cm). Below 43 cm (extrapolated depth), the ^{210}Pb activities increase to 0.71 DPM/g in section 90-91 cm (extrapolated depth 80.5-115.5 cm), then decrease to 0.23 DPM/g in section 200-201 cm, and again increase to 1.16 DPM/g at the bottom of the core (Appendix B)

Unsupported ^{210}Pb (or excess ^{210}Pb) is the amount of the ^{210}Pb isotope that is in excess to the background ^{210}Pb (background also called supported ^{210}Pb) produced in the sediments by ^{226}Ra. The unsupported ^{210}Pb is assumed to be from direct atmospheric deposition of ^{210}Pb plus the import of ^{210}Pb from the watershed and adjacent sediments.

^{226}Ra was measured in Core D at 0.23, 0.20 and 0.54 DPM/g in sections 8-9 cm, 25-26 cm and 90-91 cm, respectively (Appendix B). The ^{210}Pb activities seen in section 8-9 cm and section 25-26 cm are significantly higher than the ^{226}Ra activities measured in the same sections, suggesting that detectable atmospheric sourced ^{210}Pb is present in this section and likely in the upper 30.5 cm (extrapolated depth) of the core. The ^{226}Ra activity in section 90-91 cm is not significantly different than the ^{210}Pb activity measured in the same section, indicating that detectable atmospheric sourced ^{210}Pb was not found in this section, and is unlikely to be found in any of the sections below 30.5 cm (extrapolated depth) of this core.

Unsupported ^{210}Pb activity in Core D was calculated by subtracting the ^{226}Ra activity of 0.23 DPM/g measured in section 8-9 cm from each total ^{210}Pb value in the upper 30.5 cm of the core (Appendix B). To apply a linear regression model of unsupported ^{210}Pb activity versus cumulative dry weight, it is assumed that the input of ^{210}Pb and the sediment accumulation rate are constant. These assumptions are not satisfied, and therefore no linear regression could be calculated.

The constant rate of supply model used to determine SAR assumes constant input of ^{210}Pb and a core that is long enough to include all of the measurable atmospheric source ^{210}Pb, (i.e., it contains a complete ^{210}Pb inventory) (Appleby and Oldfield, 1978). Although it appears that the ^{210}Pb background level may have been achieved in section 90-91 cm, the assumption of a constant input of ^{210}Pb is not satisfied due to the irregular ^{210}Pb profile, and therefore no model of SAR can be applied to the dataset.

4.1.2 Core D Interpretation

The low unsupported ^{210}Pb activity found in Core D may be due to hydrodynamic activity, or bioturbation, which strips the sediment of organic matter for which ^{210}Pb has an affinity. Detectable atmospheric sourced ^{210}Pb was found in the upper 30.5 cm (extrapolated depth). It is impossible to confidently determine the date of deposition of any sediments in this core interval, other than to say that above 30.5 cm depth they appear to be less than 67 years old (3 half-lives of ^{210}Pb), the maximum age that can be estimated in this core. Below 30.5 cm of the core, the sediments are likely to be older than 67 years. Despite the unfortunate situation where no age-depth model could be calculated, the analytical quality of radioisotope data

(based upon the recovery of spike, the results of repeat analyses, CRM and blanks) is considered good.

4.1.3 Core E Results

Core E shows an irregular ^{210}Pb profile. The ^{210}Pb activity generally increases from 0.61 DPM/g in the uppermost section (extrapolated depth 0-1.5 cm) to 0.80 DPM in section 8-9 cm (extrapolated depth 7.5-9.5 cm), then it decreases to 0.24 DPM/g in section 25-26 cm (extrapolated depth 23-30.5 cm). Below 30.5 cm (extrapolated depth), the ^{210}Pb activity increases again to 0.64 DPM/g in section 90-91 cm (extrapolated depth 80.5-105.5 cm) and then decreases to 0.29 DPM/g at the bottom of the core (Appendix B).

^{226}Ra was measured in Core E at 0.22, 0.42 and 0.52 DPM/g in sections 8-9 cm, 50-51 cm and 90-91 cm, respectively (Appendix B). The ^{210}Pb activity (0.80 DPM/g) seen in section 8-9 cm is significantly higher than the ^{226}Pb activity measured in the same section, suggesting that detectable atmospheric sourced ^{210}Pb is present in this section and likely in the upper 23 cm (extrapolated depth) of the core. The ^{226}Ra activities in section 50-51 cm and section 90-91 cm are not significantly different than the ^{210}Pb activities measured in the same sections, indicating that detectable atmospheric sourced ^{210}Pb was not found in those two sections, and is unlikely to be found in any of the sections below 23 cm (extrapolated depth) of this core.

The unsupported ^{210}Pb activity was calculated by subtracting the ^{226}Ra activity of 0.22 DPM/g measured in section 8-9 cm from each total ^{210}Pb value in the upper 23 cm of the core (Appendix B). The input of ^{210}Pb and the sediment accumulation rate were not found to be constant, and therefore, a linear regression model of unsupported ^{210}Pb activity versus cumulative dry weight could not be calculated.

Although it appears that the ^{210}Pb background level may have been achieved in section 50-51 cm from core E, the assumption of a constant input of ^{210}Pb is not satisfied due to the irregular ^{210}Pb profile, and therefore no model of SAR can be applied to the dataset.

4.1.4 Core E Interpretation

The low unsupported ^{210}Pb activity found in Core E may be due to hydrodynamic activity, or bioturbation, which strips the sediment of organic matter for which ^{210}Pb has an affinity. Detectable atmospheric sourced ^{210}Pb was found in the upper 23 cm (extrapolated depth). It is impossible to confidently determine the date of deposition of any sediments in this core interval, other than to say they appear to be less than 45 years old (2 half-lives of ^{210}Pb), the maximum age that can be estimated in this core. Below 23 cm of the core, the sediments are likely to be older than 45 years. Despite the unfortunate situation where not age-depth model could be calculated, the analytical quality of radioisotope data (based upon the recovery of spike, the results of repeat analyses, CRM and blanks) is considered good.

4.1.5 Core F Results

This core shows an irregular ^{210}Pb profile. The ^{210}Pb activities vary between 0.58-1.01 DPM/g in the upper 18 cm (extrapolated depth) of the core, then vary between 0.33-0.46 DPM/g in the core interval of 18-180.5 cm (extrapolated depths). Below 180.5 cm (extrapolated depth), the ^{210}Pb activities vary between 0.61-0.84 DPM/g (Appendix B).

^{226}Ra was measured at 0.26, 0.40 and 0.31 DPM/g in sections 8-9 cm, 25-26 cm and 90-91 cm, respectively (Appendix B). The ^{210}Pb activity (0.70 DPM/g) seen in section 8-9 cm is significantly higher than the ^{226}Ra activity measured in the same section, suggesting that

detectable atmospheric sourced ^{210}Pb is present in this section and likely in the upper 18 cm (extrapolated depth) of the core. The ^{226}Pb activities in section 25-26 cm and section 90-91 cm are not significantly different than the ^{210}Pb activities measured in the same sections, indicating that detectable atmospheric sourced ^{210}Pb was not found in those two sections, and is unlikely to be found in any of the sections below 18 cm (extrapolated depth) of this core.

The unsupported ^{210}Pb activity was calculated by subtracting the ^{226}Pb activity of 0.26 DPM/g measured in section 8-9 cm from each total ^{210}Pb value in the upper 18 cm of the core (Appendix B). The input of ^{210}Pb and the sediment accumulation rate were not found to be constant, and therefore, a linear regression model of unsupported ^{210}Pb activity versus cumulative dry weight could not be calculated.

It is likely that the ^{210}Pb background level was achieved in section 25-26 cm, the assumption of a constant input of ^{210}Pb is not satisfied due to the irregular ^{210}Pb profile, and therefore no model of SAR can be applied to the dataset.

4.1.6 Core F Interpretation

The low unsupported ^{210}Pb activity may be due to hydrodynamic activity which strips the sediment of organic matter for which ^{210}Pb has an affinity. Detectable atmospheric sourced ^{210}Pb was found in the upper 18 cm (extrapolated depth). It is impossible to confidently determine the date of deposition of any sediments in this core interval, other than to say they appear to be less than 45 years old (2 half-lives of ^{210}Pb), the maximum age that can be estimated in this core. Below 18 cm of the core, the sediments are likely to be older than 45 years. Nonetheless, overall, the analytical quality of radioisotope data (based upon the recovery of spike, the results of repeat analyses, CRM and blanks) is considered good.

4.2 Core Analysis

4.2.1 Sedimentary Facies

The stratigraphic interval intersected by the nine vibracores across the harbour indicate that the uppermost ca. 3 m of intertidal sediments comprises five depositional units / sedimentary facies (Table 2; Appendices C and D). Facies 1 is clast-supported calci-gravel, that is interpreted to have been deposited by erosive events that winnowed fine-grained material and concentrated shells (Fig. 2A). An alternative interpretation for the calci-gravel is that is represents rapid faunal die-off events. Facies 2 comprises rippled to cross bedded sand, interpreted to be the product of migrating subaqueous dunes and ripples with minor wave influence (Fig. 2B). Facies 3 consists of bioturbated sand, gravelly silty sand, or silty sand, produced by thorough mixing of sandy substrates (i.e., Facies 2; Fig. 2C). Facies 4 is composed of laminated to rippled silt, resulting from migration of silty subaqueous ripples under high-concentrations of mud in the water column (Fig. 2D). Finally, Facies 5 is bioturbated sandy silt and silt, which is the product of thorough biogenic mixing of silty substrates (i.e., Facies 4; Fig. 2E).

4.2.2 Grain Size Distribution

Analysis of sediment samples from vibracores shows that grain size varies from sand to silt; the fine fraction is not composed of grains smaller than 3.9 μm (Figs. 3 and 4; Appendix D). Cumulative proportion and frequency distribution plots demonstrate that most of the sediment has a bimodal grain size distribution with a fine-silt and coarse-silt component, or a coarse silt and sand component (Appendix D). Stratigraphic columns of all cores show

alternations between beds of calci-gravel (shell layers), sand and silty sand, as well as sandy silt and silt (Figs. 3 and 4; Appendix C).

4.2.3 Loss-on-Ignition

Analysis of sediment using LOI shows a range of values from 0.9 to 9.1%. Large LOI values are usually associated with finer grained sediment, and smaller LOI values are characteristic of coarser sediment. There was not an obvious relationship between LOI in cores and the location of the core within the estuary, nor was there a clear stratigraphic pattern.

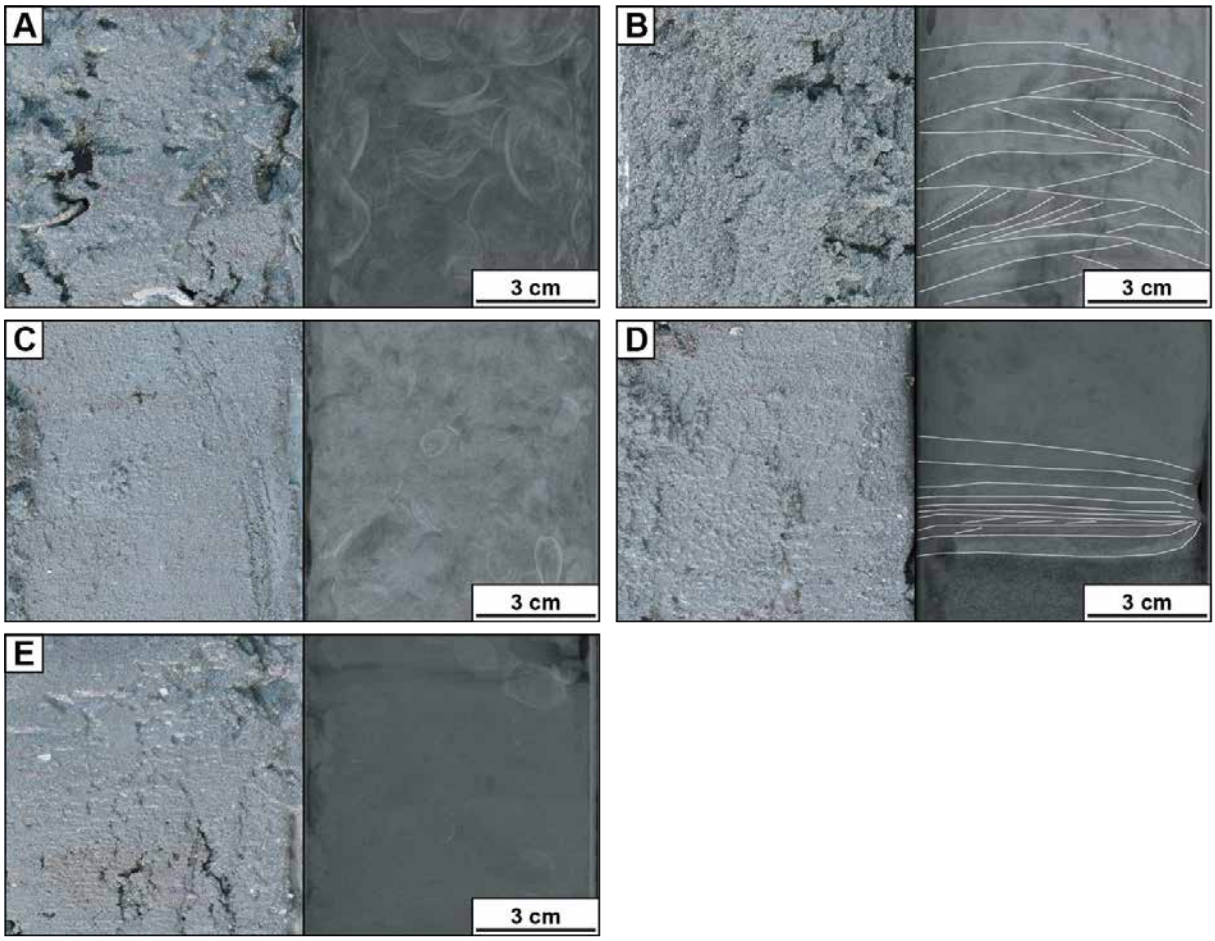

Figure 2: Core photographs and x-radiographs of the facies encountered in Ōhiwa Harbour Cores. (A) Uncemented bivalve-gastropod clast supported calci-gravel with mud matrix (Facies 1) from Core A, 0.16 m to 0.23 m. (B) Rippled sand (Facies 2) from Core F, 1.44 m to 1.51 m. (C) Bioturbated muddy sand with scattered shell fragments (Facies 3) from Core C, 1.14 m to 1.20 m. (D) Laminated to rippled mud (Facies 4) from Core A, 1.46 m to 1.53 m. (E) Bioturbated sandy mud with shell fragments (Facies 5) from Core A, 0.54 m to 0.61 m.

Table 2: Facies classification scheme.

Facies	Thickness	Grain Size	Physical Structures	Bioturbation Intensity	Accessories	Process Interpretation
Facies 1: Clast Supported Calci-gravel	2-35 cm	More than 50% shells that are >2 mm. May have sand or silt matrix. Generally, clast supported.	Rare faint bedding.	BI 5-6	Predominantly comprises bivalve shells, with subordinate gastropods.	Erosive events that winnow matrix material and condense shells OR rapid faunal die-off faunal events.
Facies 2: Rippled to Cross Bedded Sand	6-130 cm	Fine sand to medium sand	Low-angle tabular cross beds, current ripples, wave ripples.	BI 0-3	None.	Migration of sandy subaqueous dunes and ripples. Minor wind-wave influence.
Facies 3: Bioturbated Sand, Gravelly Muddy Sand, and Muddy Sand	16-44 cm	Very fine sand to coarse sand	None preserved.	BI 5-6	Scattered bivalve and gastropod shells, shell layers less than 50% shell material, comminated plant debris.	Long-term reworking of sandy substrates.
Facies 4: Laminated to Rippled Mud	14-35 cm	Fine silt to coarse silt.	Current ripples, wavy-undulatory laminae, planar parallel lamination.	BI 0-2	None.	Flows with high concentrations of mud. Migrating ripples (rippled) or quasi-laminar plug flows (laminated).
Facies 5: Bioturbated Sandy Mud and Mud	7-84 cm	Fine silt to coarse silt.	Rare normal graded laminae.	BI 4-6	Scattered bivalve and gastropod shells, shell layers less than 50% shell material, comminated plant debris.	Long-term reworking of muddy substrates.

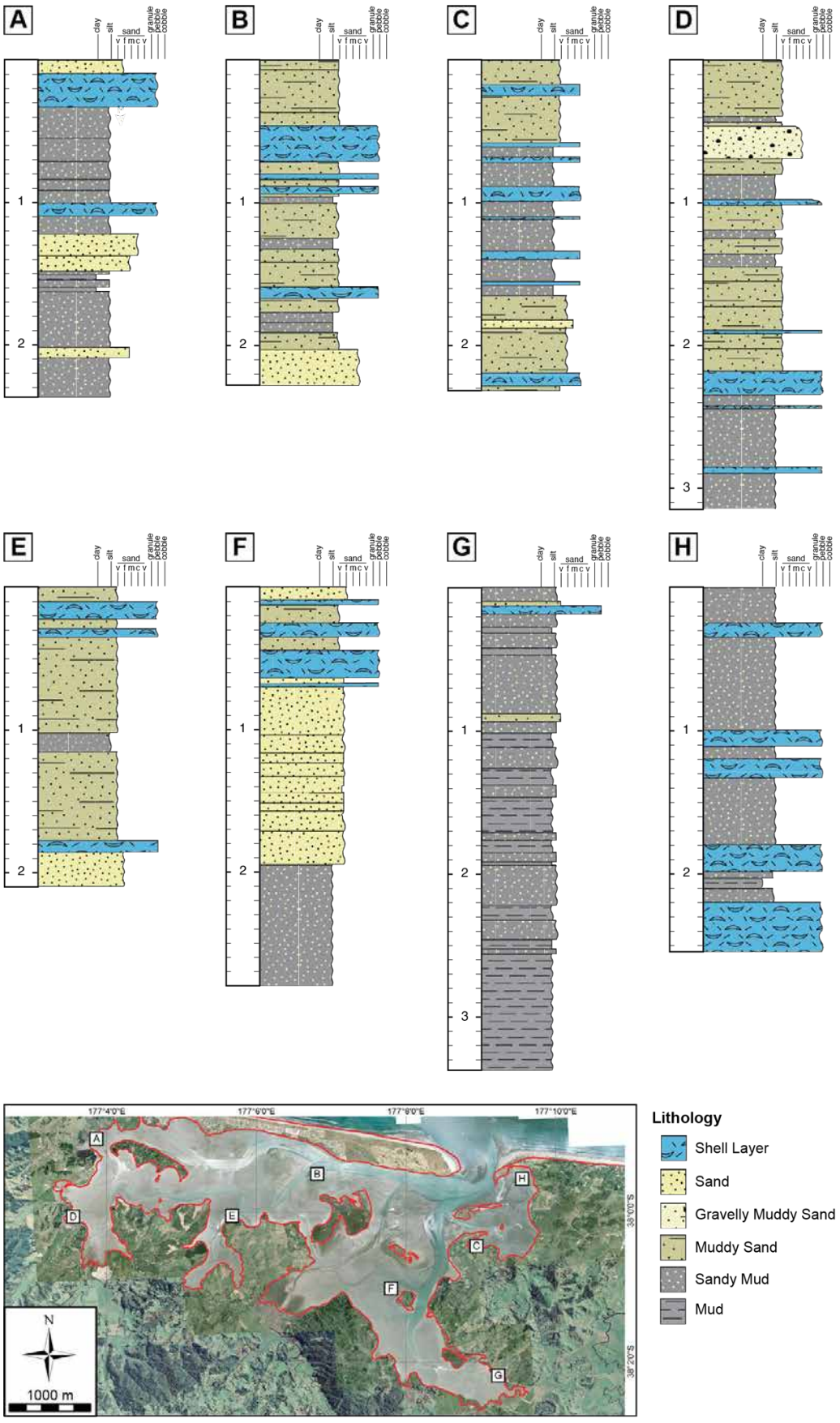

Figure 3: Simplified core lithologs from the nine vibracores collected across the harbour. See Appendix C for detailed logs.

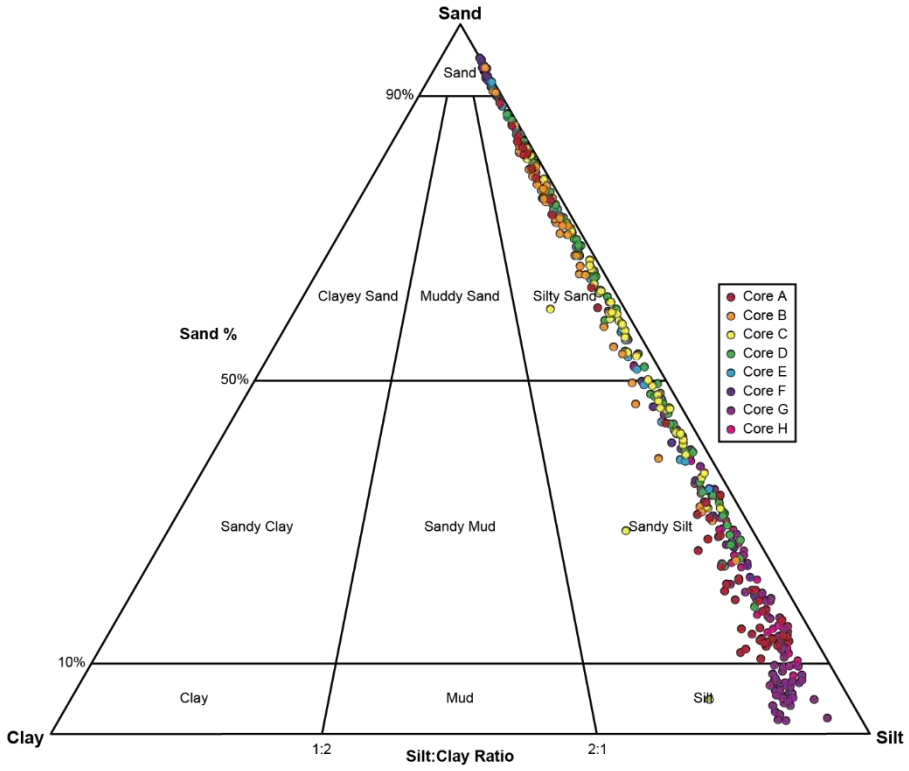

Figure 4: Sand-silt-clay ternary plot showing the grain size characteristics of vibracores.

4.4 Surface Sediment Analysis

4.4.1 Grain Size Distribution

Similar to the vibracores, surface sediment samples show a grain size that varies from sand to sandy silt, with a fine fraction comprising silt (Fig. 4; Appendix E). Cumulative proportion and frequency distribution plots indicate that most of the sediment has a bimodal grain size distribution with a fine-silt and coarse-silt component, or a coarse-silt and sand component (Appendix E).

Maps of mean grain size show that the perimeter of the harbour (e.g., sites A, D, G) has an overall finer and more narrow range of grain sizes than sites located in the central portion of the harbour (e.g., sites B, E, F) (Appendix F). The proportion of mud maps show the same pattern, with higher proportions of silt along the harbour perimeter relative to the harbour centre (Appendix F).

4.4.2 Loss-on-Ignition

Analysis of surface sediment for LOI yielded a range of 1.3 to 6.2% (Fig. 5; Appendix F). Large LOI values were associated with fine grained sediments, with small LOI typical of coarse-grained sediments. This general pattern is reflected in the spatial distribution of LOI, with sites on the perimeter having higher mean values (e.g., sites A, D, G). In particular, site D which is located near the mussel farm showed the highest overall LOI (Appendix F).

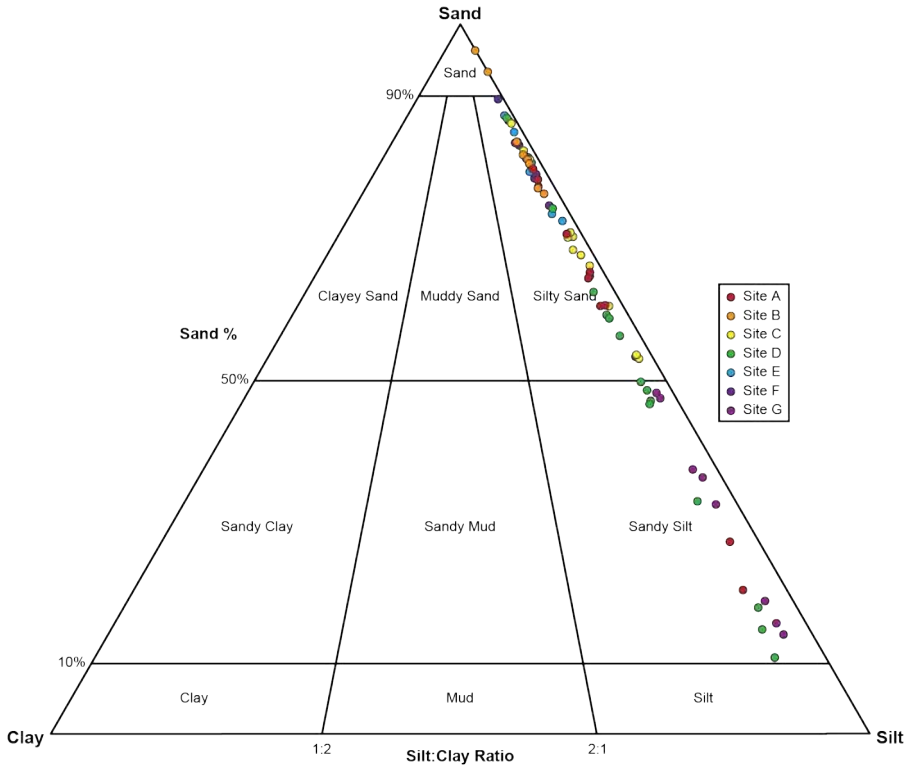

Figure 5: Sand-silt-clay ternary plot showing the grain size characteristics of surface sediments.

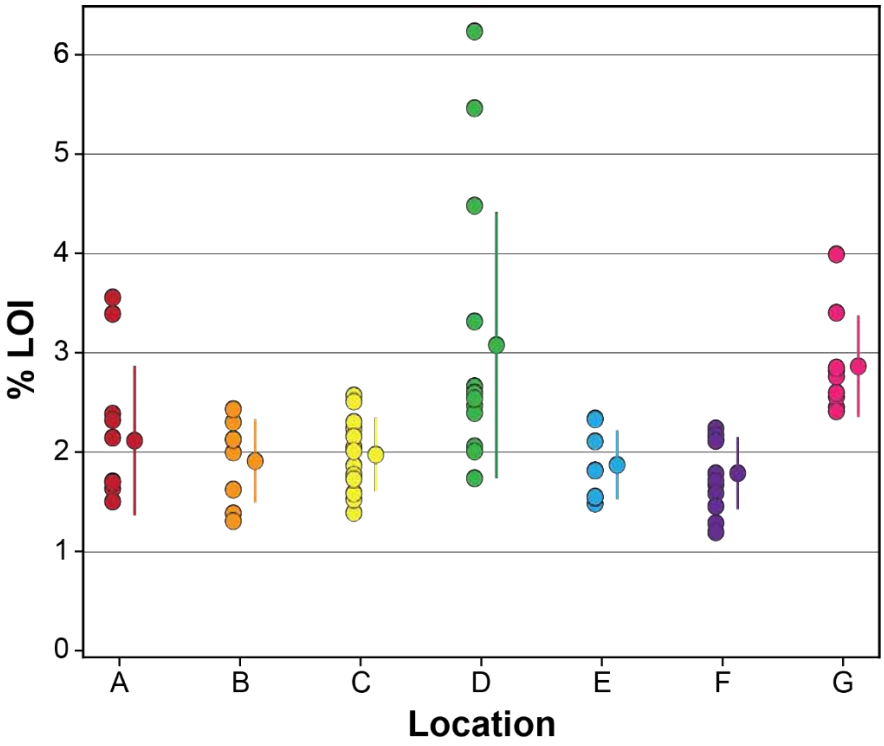

Figure 6: Percentage LOI data from each study site, along with the mean and standard deviation.

5. Discussion

5.1 Sediment Mixing Makes Radionuclide Analysis Unsuitable

The inability to determine contemporary or recent-historical SAR using ^{210}Pb and ^{226}Ra in Ōhiwa Harbour is likely the result of two factors: 1) Hydrodynamic mixing of near surface sediment in the harbour, and 2) biotubation of the sediment column. Within a surface mixed layer – the depth to which sediment is re-worked, primarily by biogenic processes – particles can be brought from the surface to depth in as little as a few months to a year (Nittrouer et al., 1984). The surface mixed layer is a zone where SAR cannot be determined.

It is well known that the barrier spits impounding Ōhiwa Harbour undergo repeated episodes of erosion and shoreline retreat that alternate with accretion and shoreline progradation (Gibb, 1977; Smith, 1976). Bryan et al. (2008) demonstrated that these events occur on decadal cycles in association with El Niños and La Niña episodes. The sedimentary environments in the lower harbour are likely to be affected by such events, as well as more regular wave activity (Richmond et al., 1984), which contributes to hydrodynamic sorting of the sedimentsand associated organic matter for which ^{210}Pb has an affinity (Keil et al., 1994). By contrast, due to the generally low-energy environmental conditions of the upper harbour, the impact of hydrodynamics in affecting the preservation of sediment organic matter and ^{210}Pb is considerably less.

Ōhiwa Harbour contains a relatively divese and plentiful community of marine invertebrates consisting of various bivalves, crustaceans, and gastropods (Richmond et al., 1984). However, the bivavles *Austrovenus stutchburyi* (cockle) and *Amphidesma astrale* (pipi) are the most conspicuous and densly populated invertebrates in the harbour (Fig. 7) (McArdle and Blackwell, 1989; Paul, 1966). The infaunal animals supply aragonite ($CaCO_3$) in the form of shell material, contribute to organic matter from faecal waste, and are a major agent of sediment reworking; Richmond et al. (1984) estimate that the surface mixed layer extends to a depth of between 20 and 30 cm and our results support that interpretation. In addition to invertebrates, algae, eel grass, salt marsh plants, and mangroves are also widespread and in some cases dense along the tidal flats (Fig. 7). Estuarine plants primarily bind the sediment together (Richmond et al., 1984), and slow or prevent physical processes from erosion, although to some degree their root systems also “rhizoturbate” the substrate. The effects of bioturbation and rhizoturbation are clearly evident in cores, with very high bioturbation intensity characterizing the bulk of the sediment column across the harbour.

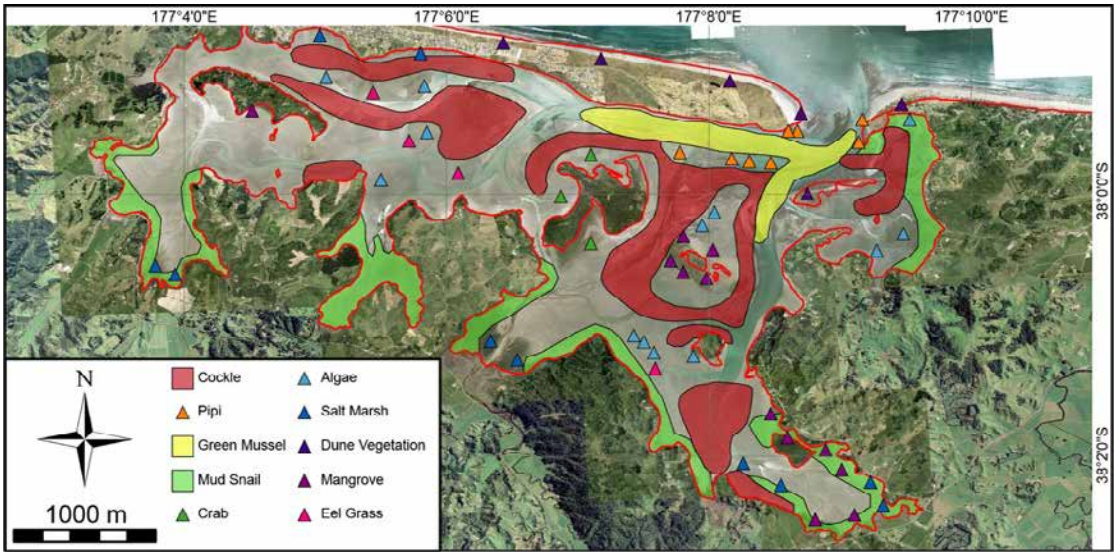

Figure 7: Major biofacies distribution map from Richmond et al. (1984)

5.2 Historical Comparison of Grain Size Distribution

The grain size of surface sediments across Ōhiwa Harbour has been mapped several times over the past five decades. Figure 8A is a map produced with the data collected by (Richmond, 1977), which shows that in 1976 the muddiest parts of the estuary were located in the southwest (up to 90% mud) and southeast (up to 56% mud). At that time the rest of the estuary was relatively sandy, having mud proportions ranging up to ca. 30%.

The BoPCRC replicated Richmond's sediment surveys in 2001 and 2010 (Stephen Park, pers. comm.), as displayed in Figure 8B and C respectively, showing that there was a general increase the proportion of mud through time. Importantly, the change in surface sediment grain size has not been the same everywhere, and some areas have become sandier through time. Overall, the maps suggest that the fringes of the estuary are the locations where changes in sediment grain size are most pronounced. The map of mean grain size of the harbour displayed in Richmond et al. (1984) and redrawn in our Figure 9 depicts a setting that predominantly comprises very fine- to coarse-grained sand, even in the upper reaches. Richmond et al. (1984)'s sand-silt-clay ternary plot shows the same pattern, with only 2 samples containing significant proportions of silt or clay.

Although the grain size data reported herein is focused around the coring sites, and therefore does not span all environments within the estuary, it supports a notion that the harbour has become muddier through time. Specifically, the margins of the harbour (sites A, D, G) are muddier compared with older maps of sediment grain size (Appendix F). The data reported herein shows that in the finest grained parts of the lagoon mud comprises up to 83-90% of the sediment. This is compared to the rest of the sampled locations where the proportion of mud seldom reaches greater than ca. 30%.

The shifts in sediment grain size over the past decades clearly demonstrates how dynamic and changing the lagoon is. We cannot isolate individual causes of grain size variation, but we can rule out the impact of any recent large-scale tectonic factors, such as earthquakes (Hayward et al., 2004). However, smaller-scale subsidence along active faults may have created accomodation which would affect the balance of marine versus land-derived sediment. Mātauranga Māori indicates that around the time of Polynesian arrival the eastern

edge of the harbour entrance was rock (Willem De Lange, pers. comm.), while it is now buried under 2-3 of sediment (Robinson, 2012). Cores described in Bell et al. (2004) suggest that the eastern harbour subsided relatively recently. Furthermore, the effects of sediment compaction under its own weight (i.e., 'autocompaction'; cf. Allen, 2000) may be causing shifts in the locations of deposition and erosion in the harbour. To date, no one has adequately characterized Ōhiwa Harbour for its autocompaction trends, but Hayward et al. (2004) estimated that compaction could vary from 20% to 50%, depending on the underlying stratigraphy. More work will be needed in this space, which is also especially relevent to backing out precise SAR values determined from radionuclide or stable carbon isotope dating.

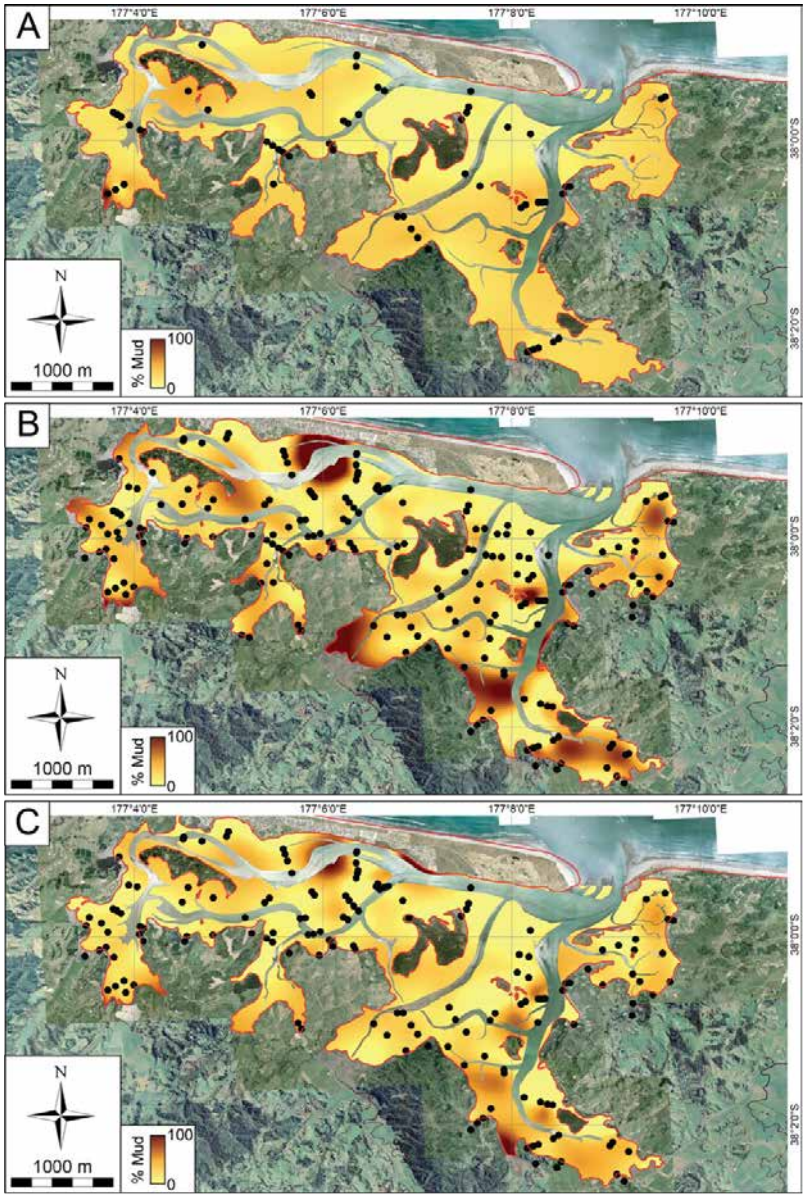

Figure 8: Surface sediment distribution maps for Ohiwa Harbour from data collected in: (A) 1978-79; (B) 2001; and (C) 2010. Data from 1978-79 is from (Richmond, 1977) and the 2001 and 2010 data is from Bay of Plenty Regional Council (Stephen Park, pers. comm.).

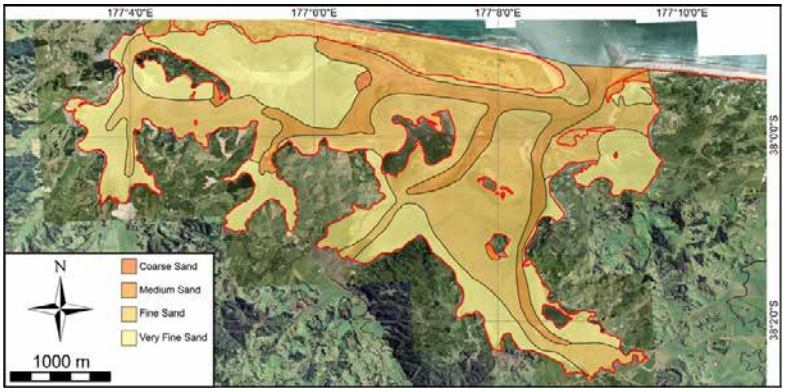

Figure 9: Map of the mean grain size of surface sediment redrawn from Richmond et al. (1984).

6. Summary and Conclusions

Vibracores, box cores, and surface sediment samples were collected from across Ōhiwa Harbour to assess sediment accumulation rates and to characterize the intertidal sediments. The core locations were chosen for their proximity to existing BoPRC sediment plates. Radionuclide activities (^{210}Pb and ^{226}Ra) were measured from three of the cores in an attempt to determine the SAR. Unfortunately, due to very low and irregular radionuclide activity down the core no linear regression or constant rate of supply model could be applied to the dataset. Notwithstanding the poor results, the quality of the data and laboratory methods was considered high. It is probable that a combination of hydrodynamic mixing and bioturbation sufficiently mixed the sediment column so as to make radionuclide analysis unsuitable for determining SAR. The only conclusions that could be drawn from the radionuclide analysis were that:

- In core D, sediments below ca. 30.5 cm are likely to be older than 67 years.
- In core E, sediments below ca. 23 cm are likely to be older than 45 years.
- In core F, sediments below ca. 18 cm are likely to be older than 45 years.

Sedimentological analysis of the vibracores and box cores indicated that the intertidal sediments within the harbour comprises five distinctive depositional units. These units will be useful for future workers interested in reconstructing the evolution of sedimentation within the harbour but require age-control before this will be possible. The units are:

- Clast-supported calci-gravel deposited by erosive events that winnowed fine-grained material and concentrated shells, or alternatively produced by rapid faunal die-off events.
- Rippled to cross bedded sand, the product of migrating subaqueous dunes and ripples with minor wave influence.
- Bioturbated sand, gravelly silty sand, or silty sand, produced by thorough mixing of sandy substrates.
- Laminated to rippled silt, resulting from migration of silty subaqueous ripples under high-concentrations of mud in the water column.
- Bioturbated sandy silt and silt, which is the product of thorough biogenic mixing of silty substrates.

Historical and new maps of the grain size of surface sediments clearly shows that, on the whole, Ōhiwa Harbour is becoming muddier through time, although in a non-linear and

complex way; in some cases, parts of the harbour have shifted towards being sandier. The perimeter of the harbour and the upper harbour are the main areas affected by a fining grain size trend.

Finally, loss-on-ignition analysis indicates that organic carbon is more concentrated in fine-grained sediment than coarser sediment. In cores there was no clear relationship between LOI and stratigraphy (depth in cores) or position of the core within the harbour. However, surface sediments display larger LOI along the perimeter of the harbour where the proportion of mud is greater.

7. Recommendations

A few key recommendations can be made based on the results of this study and gaps discovered during data collection and analysis:

- Longer-term (decades–millennia) SAR should be determined by carbon-dating the abundant shell material contained within cores.
- In combination with the carbon-dating of shells, an assessment of sediment autocompaction will help determine the causes of sedimentation and erosion in the harbour.
- Repeat sediment surveys of Richmond (1977)'s sites should be undertaken at more regular intervals. A minimum of one survey every 5 years is suggested.

8. Acknowledgements

This research was funded by Bay of Plenty Regional Council, under the advice of Stephen Park. Thanks to Prof. Karin Bryan for project set up and A/Prof. Kura Paul-Burke for liaising with the local community and iwi. Thank you to Ngāti Awa for sharing mātauranga Māori that helped understanding the context for the study, and which was used to determine appropriate sampling locations. In particular, Stevie Kloch contributed significantly to coring in the Kutarere area. Thank you Ben Stewart, Ben Roche, and Chris Morcom for assistance in the field. Holly Harvey-Wishart and Annette Rogers are acknowledged for work on grain size and loss on ignition analysis. Flett Research Limited undertook the radionuclide analysis and interpretation. Finally, thank you Dr. Willem De Lange for internal review of the report.

9. References

1991. Resource Management Act, New Zealand, pp. 835.

Allen, J.R.L., 2000. Holocene coastal lowlands: autocompaction and the uncertain ground. In: K. Pye and J.R.L. Allen (Editors), Coastal and estuarine environments: sedimentology, geomorphology and geoarchaeology. The Geological Society, London, pp. 239-252.

Anderson, M.R., Ford, R.B., Feary, D.A. and Honeywill, C., 2004. Quantitative measures of sedimentation in an estuarine system and its relationship with intertidal soft-sediment infauna. Marine Ecological Progress Series, 272: 33-48.

Appleby, P.G., 1998. Dating recent sediments by 210Pb: problems and solutions, Proceedings of the 2nd NKS/EKO-1 Seminar, Helsinki, Finland, pp. 7-24.

Appleby, P.G. and Oldfield, F., 1978. The calculation of lead-210 dates assuming a constant rate of supply of unsupported 210Pb to the sediment. Catena, 5(1): 1-8. 10.1016/s0341-8162(78)80002-2.

Barsanti, M., Garcia-Tenorio, R., Schirone, A., Rozmaric, M., Ruiz-Fernández, A.C., Sanchez-Cabeza, J.A., Delbono, I., Conte, F., De Oliveira Godoy, J.M., Heijnis, H., Eriksson, M., Hatje, V., Laissaoui, A., Nguyen, H.Q., Okuku, E., Al-Rousan, S.A., Uddin, S., Yii, M.W. and Osvath, I., 2020. Challenges and limitations of the 210Pb sediment dating method: Results from an IAEA modelling interlaboratory comparison exercise. Quaternary Geochronology, 59: 101093. 10.1016/j.quageo.2020.101093.

Basher, L.R., 2013. Erosion processes and their control in New Zealand. In: J. Dymond (Editor), Ecosystem services in New Zealand – conditions and trends, pp. 363-374.

Beanland, S. and Berryman, K.R., 1992. Holocene coastal evolution in a continental rift setting: Bay of Plenty, New Zealand. Quaternary International, 15/16: 151-158.

Bell, R.G., Goff, J., Downes, G., Berryman, K., Walters, R.A., Chagué-Goff, C., Barnes, P. and Wright, I., 2004. Tsunami hazard for the Bay of Plenty and eastern Coromandel Peninsula, NIWA, Hamilton, New Zealand.

Bentley, S.J., Swales, A., Pyenson, B. and Dawe, J., 2014. Sedimentation, bioturbation, and sedimentary fabric evolution on a modern mesotidal mudflat: A multi-tracer study of processes, rates, and scales. Estuarine, Coastal and Shelf Science, 141: 58-68. 10.1016/j.ecss.2014.02.004.

Blott, S.J. and Pye, K., 2001. GRADISTAT: a grain size distribution and statistics package for the analysis of unconsolidated sediments. Earth Surface Processes and Landforms, 26: 1237-1248.

Bryan, K.R., Kench, P.S. and Hart, D.E., 2008. Multi-decadal coastal change in New Zealand: evidence, mechanisms and implications. New Zealand Geographer, 64: 117-128. 10.1111/j.1745-7939.2008.00135.

Eakins, J.D. and Morrison, R.T., 1978. A new procedure for the determination of lead-210 in lake and marine sediments. International Journal of Applied Radiation and Isotopes, 29(9-10): 531-536.

Folk, R.L. and Ward, W.C., 1957. Brazos River bar: A study in the significance of grain size parameters. Journal of Sedimentary Petrology, 27: 3-26.

Freestone, H.J., 1976. Report of a full cycle tidal gaugin carried out at the Ohiwa Harbour entrance, 6 April 1976, Ministry of Works and Development, Rotorura, New Zealand.

Gibb, J.G., 1977. Late Quaternary sedimentary processes at Ohiwa Harbour, eastern Bay of Plenty with special reference to property loss on Ohiwa Spit, Ministry of Works and Development, Wellington, New Zealand.

Harpur, A.H., 2016. Anthropogenic influences on the sedimentary evolution of the Coromandel Harbour, University of Waikato, Hamilton, New Zealand, 199 pp.

Hayward, B.W., Cochran, U., Southall, K., Wiggins, E., Grenfell, H.R., Sabaa, A., Shane, P.R. and Gehrels, R., 2004. Micropalaeontological evidence for the Holocene earthquake history of the eastern Bay of Plenty, New Zealand, and a new index for determining the land elevation record. Quaternary Science Reviews, 23(14-15): 1651-1667. 10.1016/j.quascirev.2004.01.010.

Healy, J., 1967. Geology of Whakatane. Whakatane Historical Review, 15: 9-26.

Healy, T.R., 1978. Some textural and mineralogical investigations of the Rangitaiki Plains foreshore and river sands, Bay of Plenty Catchment Commission, Whakatane, New Zealand.

Hemmingsen, M.A., 2001. Radiocarbon age for estuarine shells from Lakelands, Lake Ellesmere (Te Waihora), New Zealand. New Zealand Journal of Marine and Freshwater Research, 35(2): 329-334. 10.1080/00288330.2001.9517003.

Hicks, D.M., Shankar, U., McKerchar, A.I., Basher, L., Jessen, M., Lynn, I. and Page, M., 2011. Suspended sediment yields from New Zealand rivers. Journal of Hydrology, 50(1): 81-142.

Huirama, M., Swales, A., Olsen, G. and Ovenden, R., 2021. Sediment accumulation rates in Waimapu, Waikareao and Tuapiro estuaries, Tauranga Harbour, National Institute of Water and Atmosphere, Hamilton, New Zealand.

Hume, T.M. and Dahm, J., 1992. An investigation of the effects of Polynesian and European land use on sedimentation on Coromandel estuaries, Department of Conservation, Hamilton, New Zealand.

Hunt, S., 2019. Summary of historic estuarine sedimentation measurements in the Waikato region and formulation of a historic baseline sedimentation rate, Waikato Regional Council, Hamilton, New Zealand.

Julian, K.A., 2006. Coastal processes influencing beach erosion at Ohope Spit, University of Waikato, Hamilton, New Zealand.

Keil, R.G., Tsamakis, E., Fuh, C.B., Giddings, J.C. and Hedges, J.I., 1994. Mineralogical and textural controls on the organic composition of coastal marine sediments: Hydrodynamic separation using SPLITT-fractionation. Geochimica et Cosmochimica Acta, 58(2): 879-893. 10.1016/0016-7037(94)90512-6.

Kennish, M.T., 2001. Marsh systems in the US: a review of anthropogenic impacts. Journal of Coastal Research, 17: 731-748.

King, D.J., Newnham, R.M., Gehrels, W.R. and Clark, K.J., 2020. Late Holocene sea-level changes and vertical land movements in New Zealand. New Zealand Journal of Geology and Geophysics, 64(1): 21-36. 10.1080/00288306.2020.1761839.

Kirk, R.M. and Lauder, G.A., 2000. Significant coastal lagoon systems in the South Island, New Zealand: coastal processes and lagoon mouth closure, Science for Conservation 146. Department of Conservation, Wellington, New Zealand.

Lambeck, K., Rouby, H., Purcell, A., Sun, Y. and Sambridge, M., 2014. Sea level and global ice volumes from the Last Glacial Maximum to the Holocene. Proc Natl Acad Sci U S A, 111(43): 15296-303. 10.1073/pnas.1411762111.

Lotze, H.K., Lenihan, H.S., Bourque, B.J., Bradbury, R.H., Cooke, R.G., Kay, M.C., Kidwell, S.M., Kirby, M.X., Peterson, C.H. and Jackson, J.B., 2006. Depletion, degradation, and recovery potential of estuaries and coastal seas. Science, 312(5781): 1806-9. 10.1126/science.1128035.

M.F.E., 2020. National Policy Statement for Freshwater Management, Ministry for the Environment — Manatū Mō Te Taiao, Wellington, New Zealand.

MacDiarmid, A., McKenzie, A., Sturman, J., Beaumont, J., Mikaloff-Fletcher, S. and Dunne, J., 2012. Assessment of anthropogenic threats to New Zealand marine habitats, Ministry of Agriculture and Forestry, Wellington, New Zealand.

MacKenzie, H., 2013. State of the Ohiwa Harbour and Catchment, Bay of Plenty Regional Council, Whakatane, New Zealand.

Manning, D.A., 1996. Middle-Late Pleistocene tephrostratigraphy of the eastern Bay of Plenty, New Zealand. Quaternary International, 34-36: 3-12. 10.1016/1040-6182(95)00064-x.

Mathieu, G.G., Biscaye, P.E., Lupton, R.A. and Hammond, D.E., 1988. System for measurement of 222Rn at low levels in natural waters. Health Physics, 55: 989-992.

McArdle, B.H. and Blackwell, R.G., 1989. Measurement of density variability in the bivalve *Chione stutchburyi* using spatial autocorrelation. Marine Ecological Progress Series, 52: 245-252.

McGlone, M.S., 1989. Report on the pollen analysis of estuarine cores from the Firth of Thames, DSIR Botany Division, Wellington, New Zealand.

Milliman, J.D., 1990. Fluvial sediment in coastal seas: flux and fate. Nature and Resources, 26: 12-22.

Murdoch, B.G., 2005. Holocene Evolution of Ohope Barrier Spit, Eastern Bay of Plenty, North Island, New Zealand, University of Waikato, Hamilton, New Zealand.

Naish, T.R., 1990. Late Holocene sedimentation and diagenesis in the Firth of Thames: bentonites in the making, University of Waikato, Hamilton, New Zealand, 154 pp.

Nichol, S.L., Augustinus, P.C., Gregory, M.R., Creese, R. and Horrocks, M., 2013. Geomorphic and Sedimentary Evidence of Human Impact on the New Zealand Coastal Landscape. Physical Geography, 21(2): 109-132. 10.1080/02723646.2000.10642702.

Nittrouer, C.A., DeMaster, D.J., McKee, B.A., Cutshall, N.H. and Larsen, I.L., 1984. The effect of sediment mixing on Pb-210 accumulation rates for the Washington continental shelf. Marine Geology, 54(3-4): 201-221. 10.1016/0025-3227(84)90038-0.

Nixon, S.W., 2012. Coastal marine eutrophication: A definition, social causes, and future concerns. Ophelia, 41(1): 199-219. 10.1080/00785236.1995.10422044.

Paola, C., Ganti, V., Mohrig, D., Runkel, A.C. and Straub, K.M., 2018. Time Not Our Time: Physical Controls on the Preservation and Measurement of Geologic Time. Annual Review of Earth and Planetary Sciences, 46(1): 409-438. 10.1146/annurev-earth-082517-010129.

Park, S., 2005. Environmental quality of Ohiwa Harbour - 2005, Bay of Plenty Regional Council, Whakatane, New Zealand.

Paul, L.J., 1966. Observations on Past and Present Distribution of Mollusc Beds in Ohiwa Harbour Bay of Plenty. New Zealand Journal of Science, 9(1): 30-&.

Paul-Burke, K., Burke, J., Te Ūpokorehe Resource Management Team, Bluett, C. and Senior, T., 2018. Using Māori knowledge to assist understandings and management of shellfish populations in Ōhiwa Harbour, Aotearoa New Zealand. New Zealand Journal of Marine and Freshwater Research, 52(4): 542-556.

Petchey, F., 2009. Dating marine shell in Oceania: Issues and prospects. In: A. Fairbairn, S. O'Connor and B. Marwick (Editors), New Directions in Archaeological Science. ANU Press, Canberra, Australia, pp. 157-172.

Richmond, B., 1977. Geomorphology and modern sediments of Ohiwa Harbour, University of Waikato, Hamilton, New Zealand.

Richmond, B.M., Nelson, C.S. and Healy, T.R., 1984. Sedimentology and evolution of Ohiwa Harbour, a barrier-impounded estuarine lagoon in Bay of Plenty. New Zealand Journal of Marine and Freshwater Research, 18: 461-478.

Robinson, B.J., 2012. Hydrodynamic impacts of tectonics in prehistoric Ohiwa Harbour, North Island, New Zealand, University of Waikato, Hamilton, New Zealand, 111 pp.

Schiel, D.R. and Howard-Williams, C., 2016. Controlling inputs from the land to sea: limit-setting, cumulative impacts and ki uta ki tai. Marine and Freshwater Research, 67(1): 57-64. 10.1071/mf14295.

Senior, T., Houghton, M., Donald, M. and Douglas, J., 2009. The Ohiwa Harbour Catchment Sediment and Mangrove Management Plan, Bay of Plenty Regional Council, Whakatane, New Zealand.

Sheffieldt, A.T., Healy, T.R. and McGlone, M.S., 1995. Infilling Rates of a Steepland Catchment Estuary, Whangamata, New Zealand. Journal of Coastal Research, 11(4): 1294-1308.

Smith, R.K., 1976. Coastline changes at Ohiwa Harbour, Ministry of Works and Development, Napier, New Zealand.

Soons, J.M. and Selby, M.J., 1992. Landforms of New Zealand 2nd Edition. Longman Paul, Hong Kong.

Straub, K.M., Duller, R.A., Foreman, B.Z. and Hajek, E.A., 2020. Buffered, Incomplete, and Shredded: The Challenges of Reading an Imperfect Stratigraphic Record. Journal of Geophysical Research: Earth Surface, 125(3): e2019JF00507. 10.1029/2019jf005079.

Swales, A., Bentley, S.J., Lovelock, C.E. and Bell, R.G., 2007. Sediment processes and mangrove-habitat expansion on a rapidly-prograding muddy coast, New Zealand, Proceedings of the 6th International Symposium on Coastal Engineering and Science of Coastal Sediment Processes New Orleans, USA, pp. 1441–1454.

Swales, A. and Hume, T.M., 1995. Sedimentation history and potential future impacts of production forestry on the Wharekawa Estuary, Coromandel Peninsula, National Institute of Water and Atmosphere, Hamilton, New Zealand.

Swales, A., Ovenden, R., Budd, R., Hawken, J., McGlone, M.S., Hermanspahn, N. and Okey, M.J., 2005. Whaingaroa (Raglan) Harbour: sedimentation and the effects of historical catchment landcover changes, National Institute of Water and Atmosphere, Hamilton, New Zealand.

Taylor, A.M. and Goldring, R., 1993. Descriptions and analysis of bioturbation and ichnofabric. Journal of the Geological Society (London), 150: 141-148.

Thrush, S.F., Hewitt, J.E., Cummings, V.J., Ellis, J.I., Hatton, C., Lohrer, A. and Norkko, A., 2004. Muddy waters: elevating sediment input to coastal and estuarine habitats. Frontiers in Ecology and the Environment, 2(6): 299-306. 10.1890/1540-9295(2004)002[0299:Mwesit]2.0.Co;2.

Townsend, M. and Lohrer, A., 2015. ANZECC guidance for estuary sedimentation, National Institue of Water and Atmosphere.

Wood, J.C., 2015. Determination of moisture content and total organic carbon within basin environments: loss-on-ignition. In: L.E. Clarke and J.M. Nield (Editors), Geomorphological Techniques (Online Edition). British Society for Geomorphology, London, United Kingdom, pp. 1-7.

Appendix A – Radionuclide Methods

Determination of Lead-210 by Measurement of Polonium-210 using Alpha Spectrometry

Sample Pre-treatment:	Dry bulk density measurement required if results will be used for soil dating. Freeze dry or oven dry as specified by client. Grind to homogeneous powder.
Preparation:	Nitric acid digestion with subsequent plating onto silver planchets.
Optional Cleanup:	Distillation at ~500 ºC
Detection:	Alpha Spectrometry (60 000 second count time)
Detection Limits: (95% confidence level)	0.5 g dry sample: MDL 0.05 DPM/g; 0.25 g dry sample: MDL 0.1 DPM/g When clean-up is required the MDL for a 0.5 g sample is 0.2 DPM/g

Determination of Radium-226 by Radon-222 Emanation

Sample Pre-treatment:	Freeze dry or oven dry as specified by client. Grind to homogeneous powder.
Preparation:	Acid digestion and Helium Strip
Detection:	Emanation / Alpha Spectrometry (60 000 second counting time)
Detection Limits: (95% confidence level)	0.5 g dry sample: MDL 0.5 DPM/g 2 g dry sample: MDL 0.1 DPM/g The lower limit will vary with weight and is determined by counting error.

Appendix B – Radionuclide Results

Core D

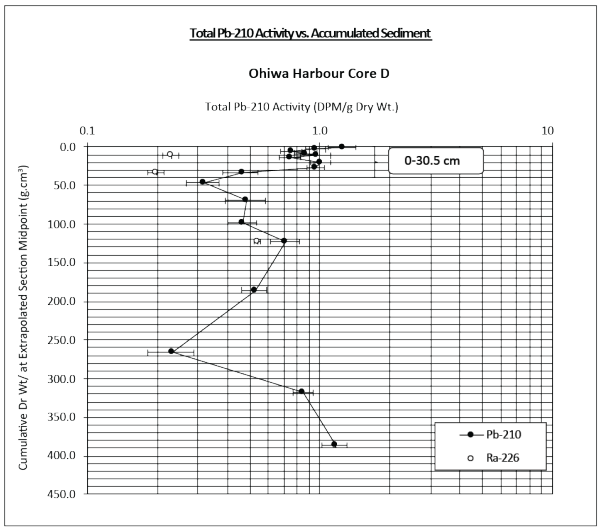

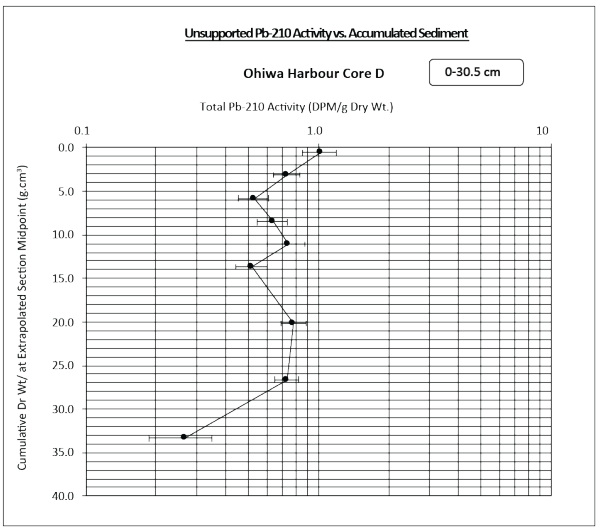

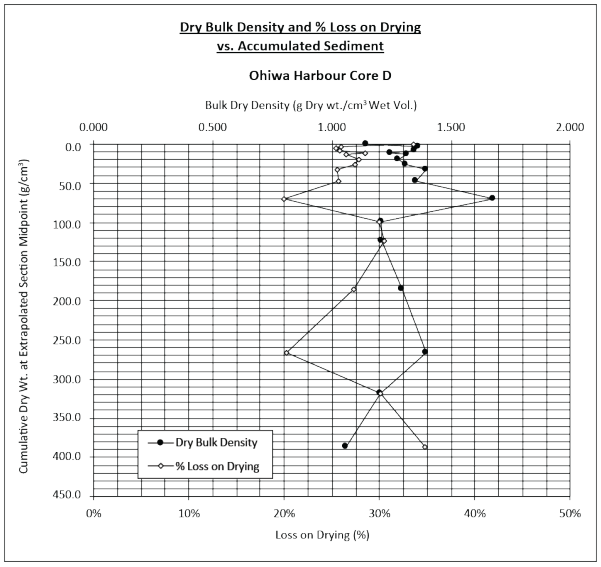

Core E

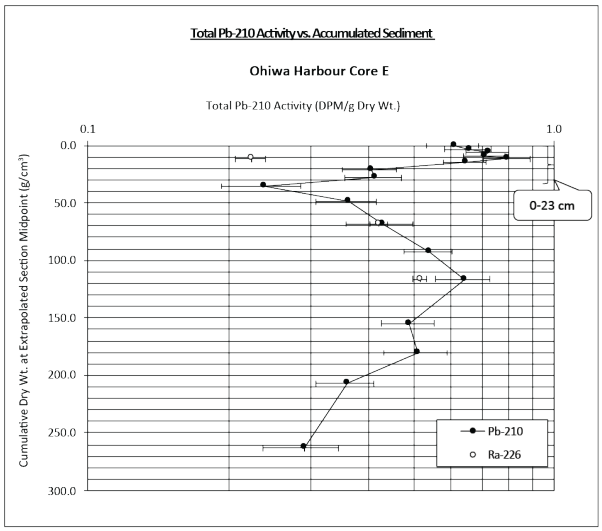
Total Pb-210 Activity vs. Accumulated Sediment
Ohiwa Harbour Core E
Total Pb-210 Activity (DPM/g Dry Wt.)
0.1
1.0
0.0
50.0
100.0
150.0
200.0
250.0
300.0
Cumulative Dry Wt. at Extrapolated Section Midpoint (g/cm²)
0-23 cm
Pb-210
Ra-226

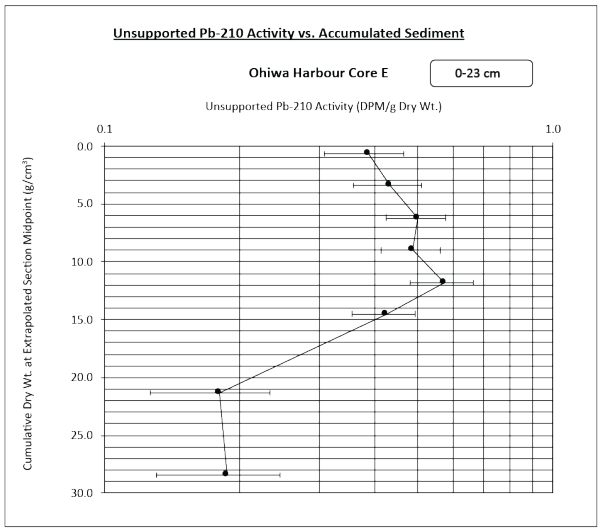
Unsupported Pb-210 Activity vs. Accumulated Sediment
Ohiwa Harbour Core E
0-23 cm
Unsupported Pb-210 Activity (DPM/g Dry Wt.)
0.1
1.0
0.0
5.0
10.0
15.0
20.0
25.0
30.0
Cumulative Dry Wt. at Extrapolated Section Midpoint (g/cm²)

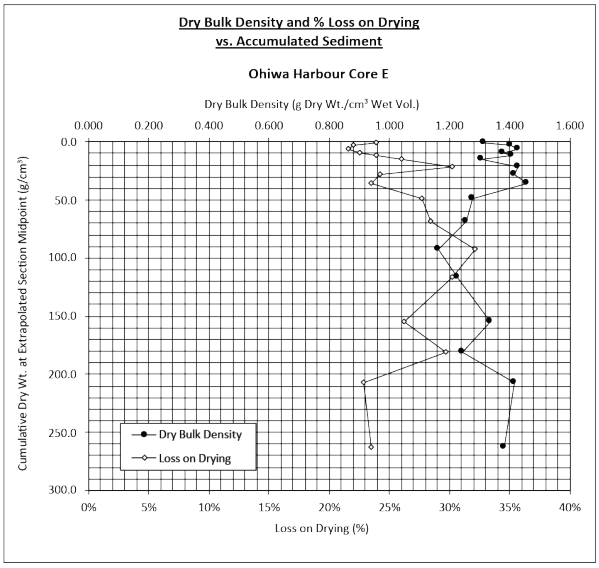
Dry Bulk Density and % Loss on Drying
vs. Accumulated Sediment
Ohiwa Harbour Core E
Dry Bulk Density (g Dry Wt./cm³ Wet Vol.)
0.000
0.200
0.400
0.600
0.800
1.000
1.200
1.400
1.600
0.0
50.0
100.0
150.0
200.0
250.0
300.0
Cumulative Dry Wt. at Extrapolated Section Midpoint (g/cm²)
Dry Bulk Density
Loss on Drying
0%
5%
10%
15%
20%
25%
30%
35%
40%
Loss on Drying (%)

Core F

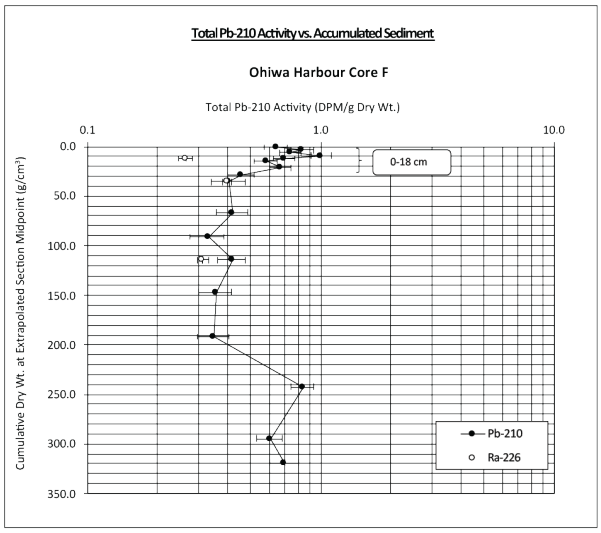
Total Pb-210 Activity vs. Accumulated Sediment
Ohiwa Harbour Core F
Total Pb-210 Activity (DPM/g Dry Wt.)
0.1
1.0
10.0
0-18 cm
Cumulative Dry Wt. at Extrapolated Section Midpoint (g/cm²)
0.0
50.0
100.0
150.0
200.0
250.0
300.0
350.0
Pb-210
Ra-226

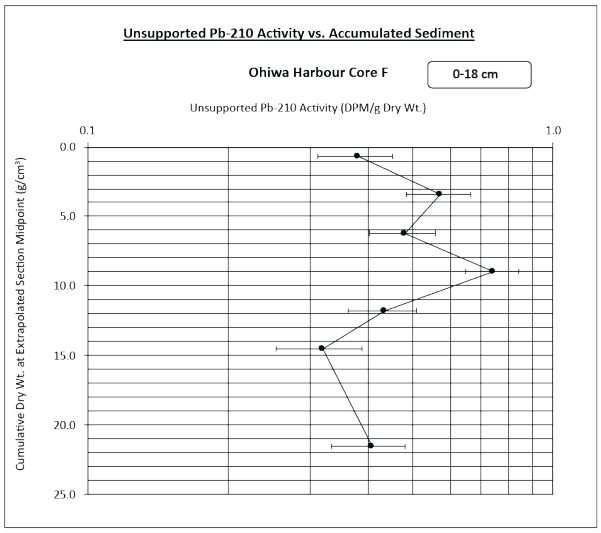
Unsupported Pb-210 Activity vs. Accumulated Sediment
Ohiwa Harbour Core F
0-18 cm
Unsupported Pb-210 Activity (DPM/g Dry Wt.)
0.1
1.0
Cumulative Dry Wt. at Extrapolated Section Midpoint (g/cm²)
0.0
5.0
10.0
15.0
20.0
25.0

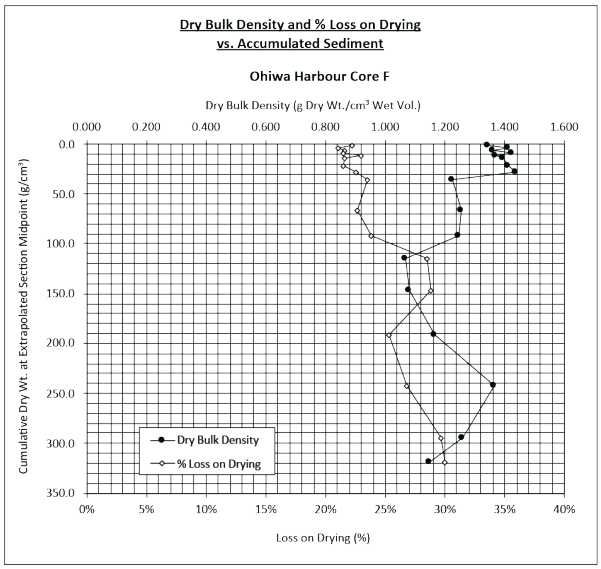
Dry Bulk Density and % Loss on Drying
vs. Accumulated Sediment
Ohiwa Harbour Core F
Dry Bulk Density (g Dry Wt./cm³ Wet Vol.)
0.000
0.200
0.400
0.600
0.800
1.000
1.200
1.400
1.600
Cumulative Dry Wt. at Extrapolated Section Midpoint (g/cm²)
0.0
50.0
100.0
150.0
200.0
250.0
300.0
350.0
Dry Bulk Density
% Loss on Drying
0%
5%
10%
15%
20%
25%
30%
35%
40%
Loss on Drying (%)

Appendix C – Lithologs

Legend

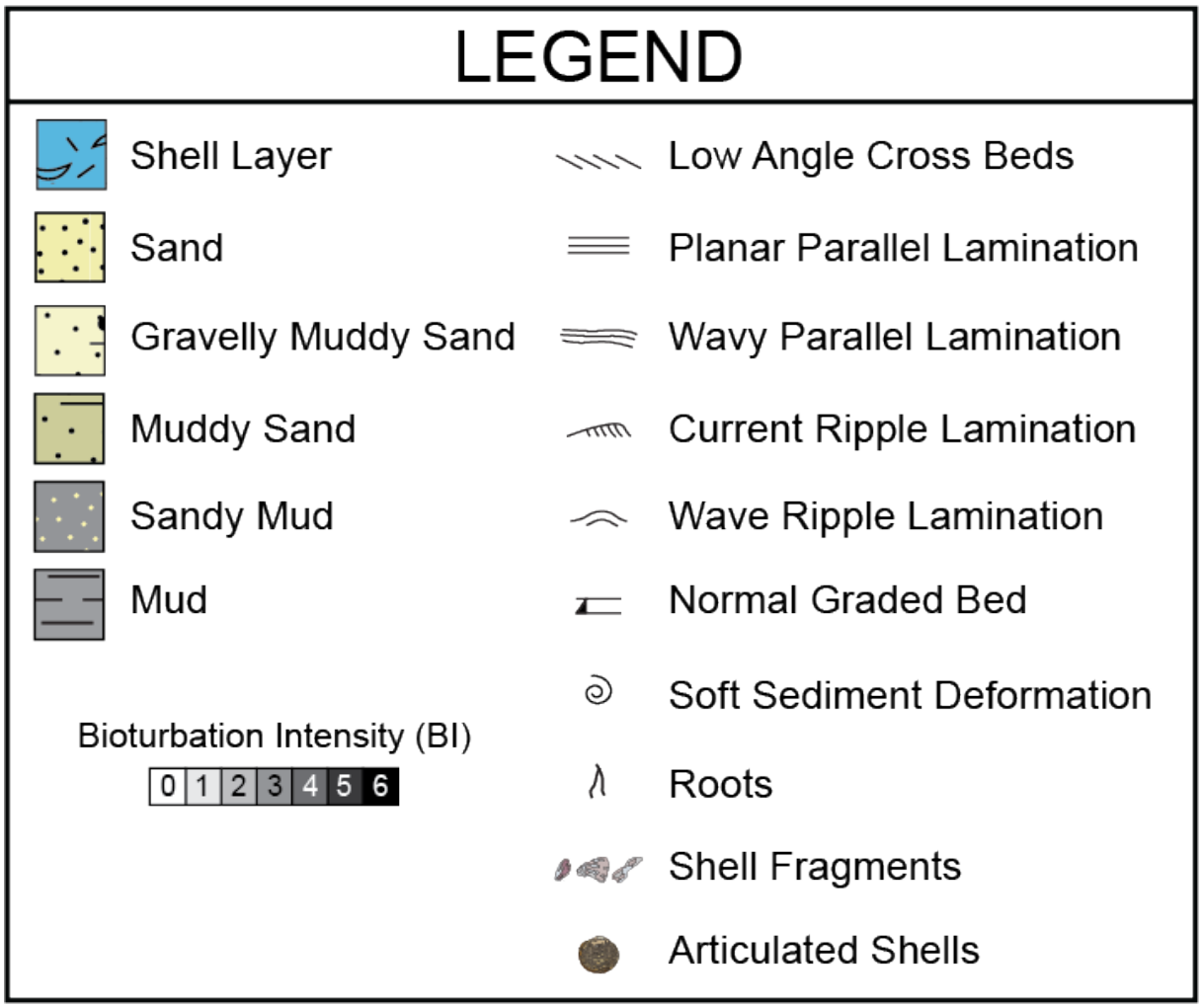

Core A

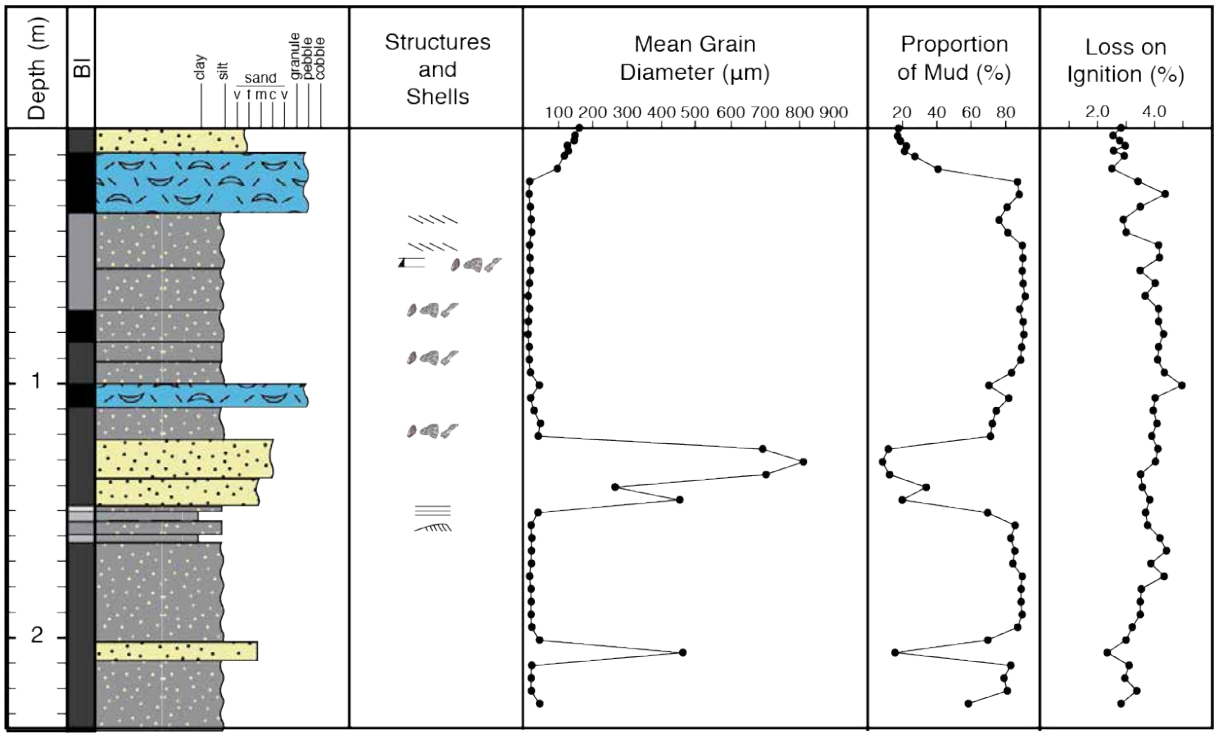
Depth (m)
BI
clay
silt
sand
v f m c v
granule
pebble
cobble
Structures and Shells
Mean Grain Diameter (µm)
100 200 300 400 500 600 700 800 900
Proportion of Mud (%)
20 40 60 80
Loss on Ignition (%)
2.0 4.0
1
2

Core B

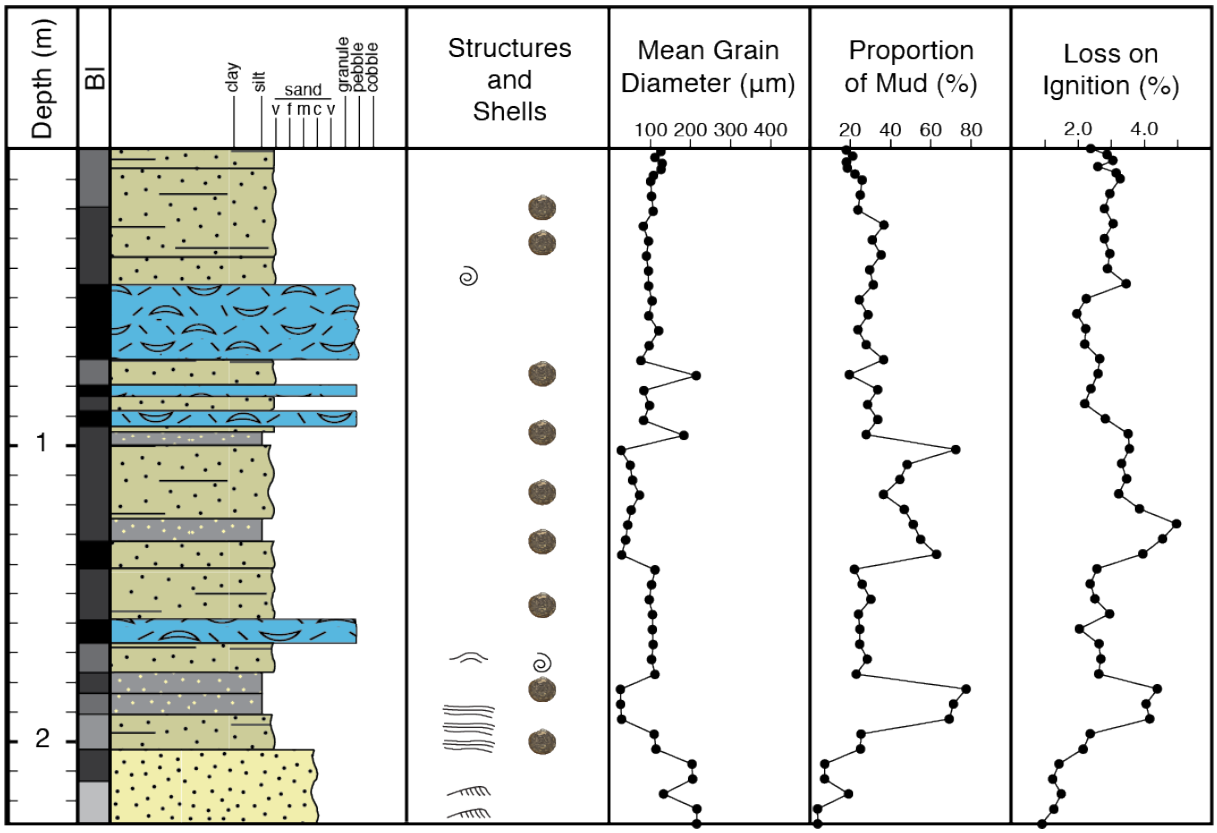
Depth (m)
BI
clay
silt
sand
v f m c v
granule
pebble
cobble
Structures and Shells
Mean Grain Diameter (µm)
100 200 300 400
Proportion of Mud (%)
20 40 60 80
Loss on Ignition (%)
2.0 4.0
1
2

Core C

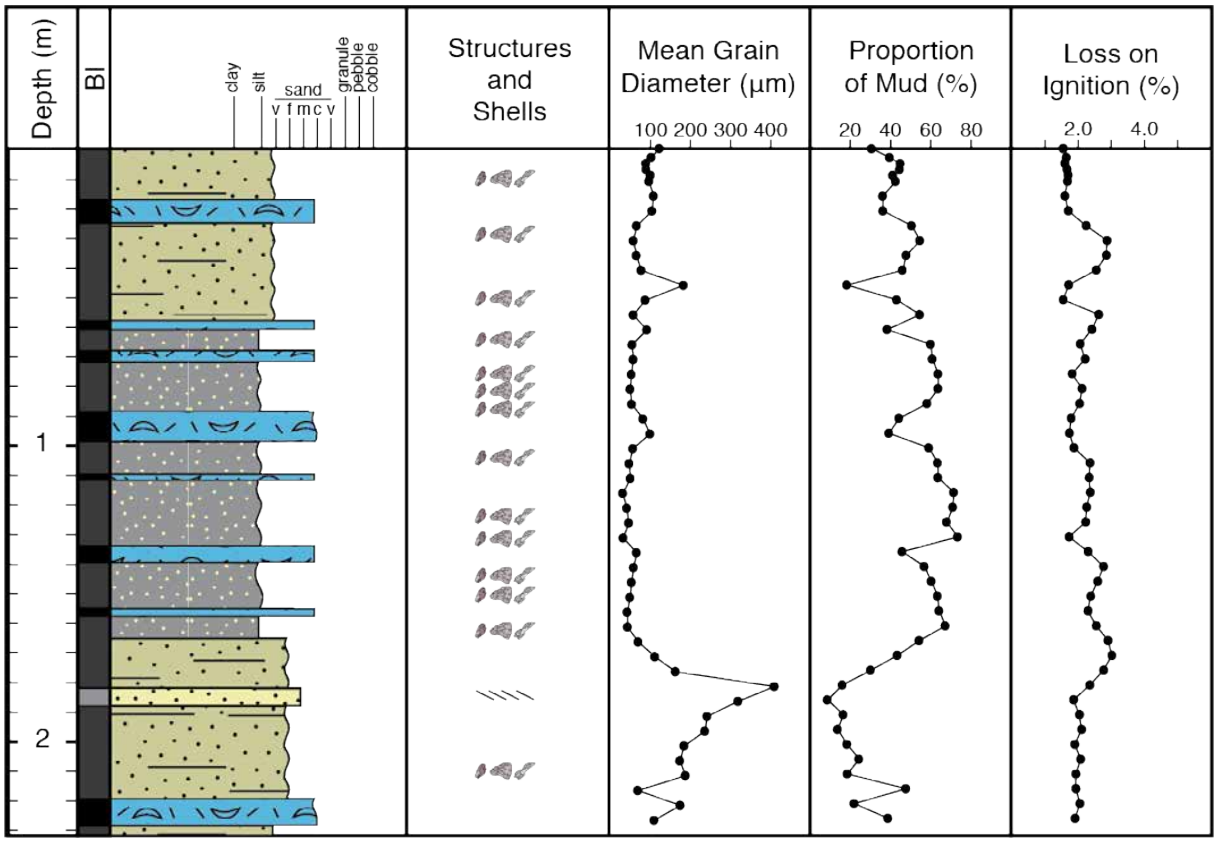
Depth (m)
BI
clay
silt
sand
v f m c v
granule
pebble
cobble
Structures and Shells
Mean Grain Diameter (µm)
100 200 300 400
Proportion of Mud (%)
20 40 60 80
Loss on Ignition (%)
2.0 4.0
1
2

Core D

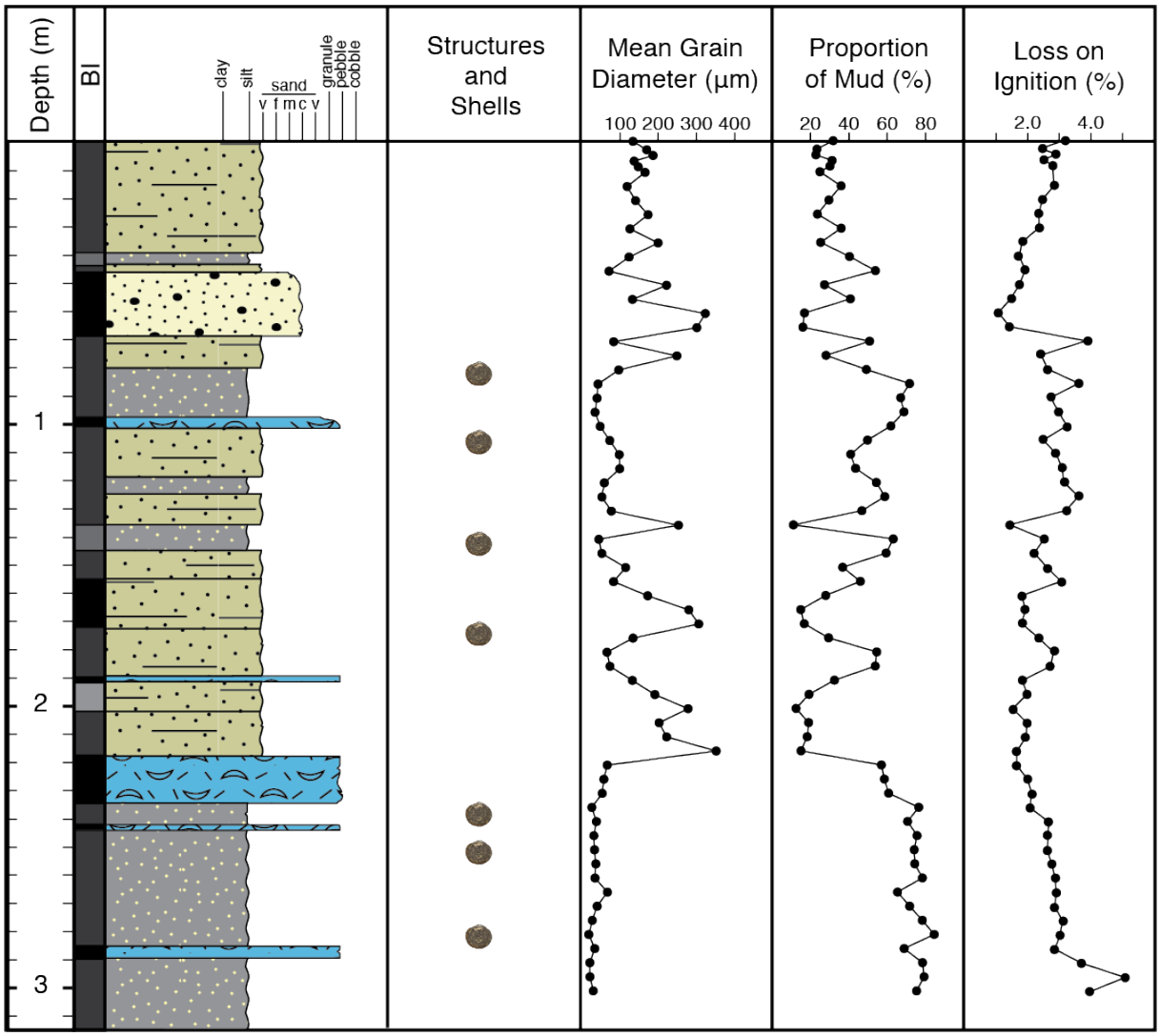
Depth (m)
BI
clay
silt
sand
v f m c v
granule
pebble
cobble
Structures and Shells
Mean Grain Diameter (µm)
100 200 300 400
Proportion of Mud (%)
20 40 60 80
Loss on Ignition (%)
2.0 4.0
1
2
3

Core E

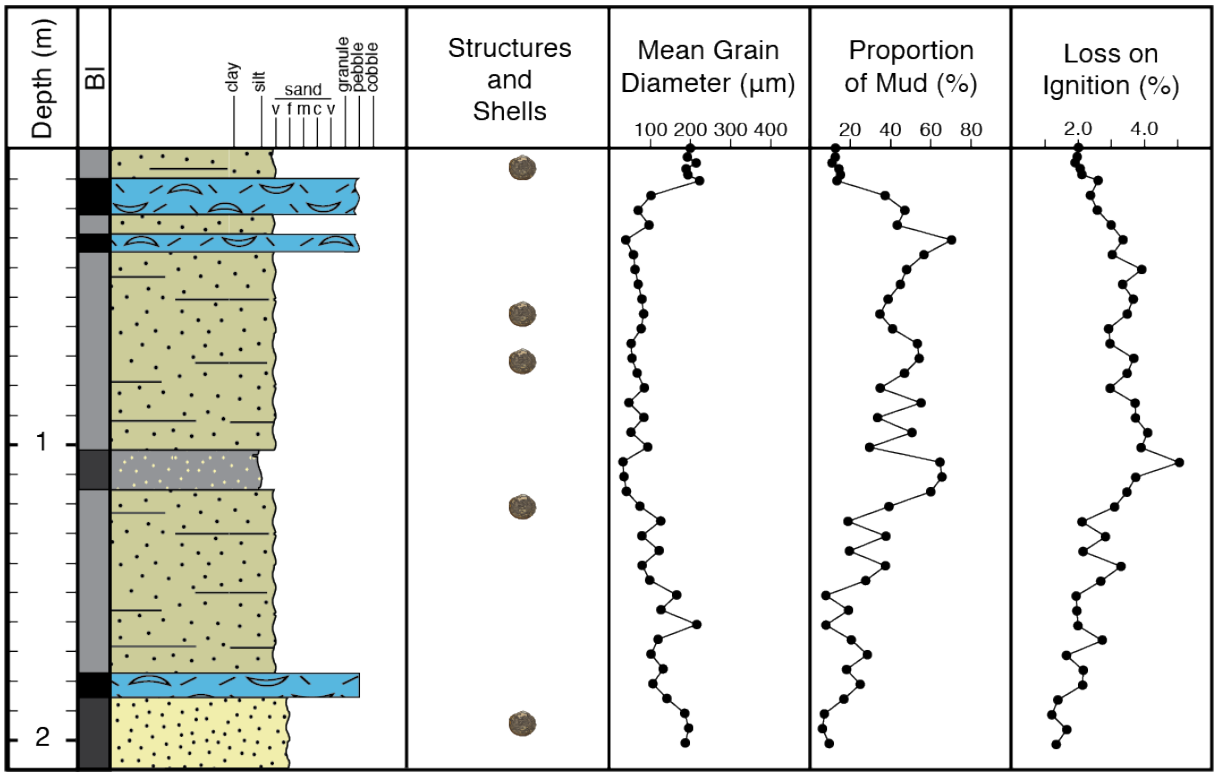
Depth (m)
BI
clay
silt
sand
v f m c v
granule
pebble
cobble
Structures and Shells
Mean Grain Diameter (µm)
100 200 300 400
Proportion of Mud (%)
20 40 60 80
Loss on Ignition (%)
2.0 4.0
1
2

Core F

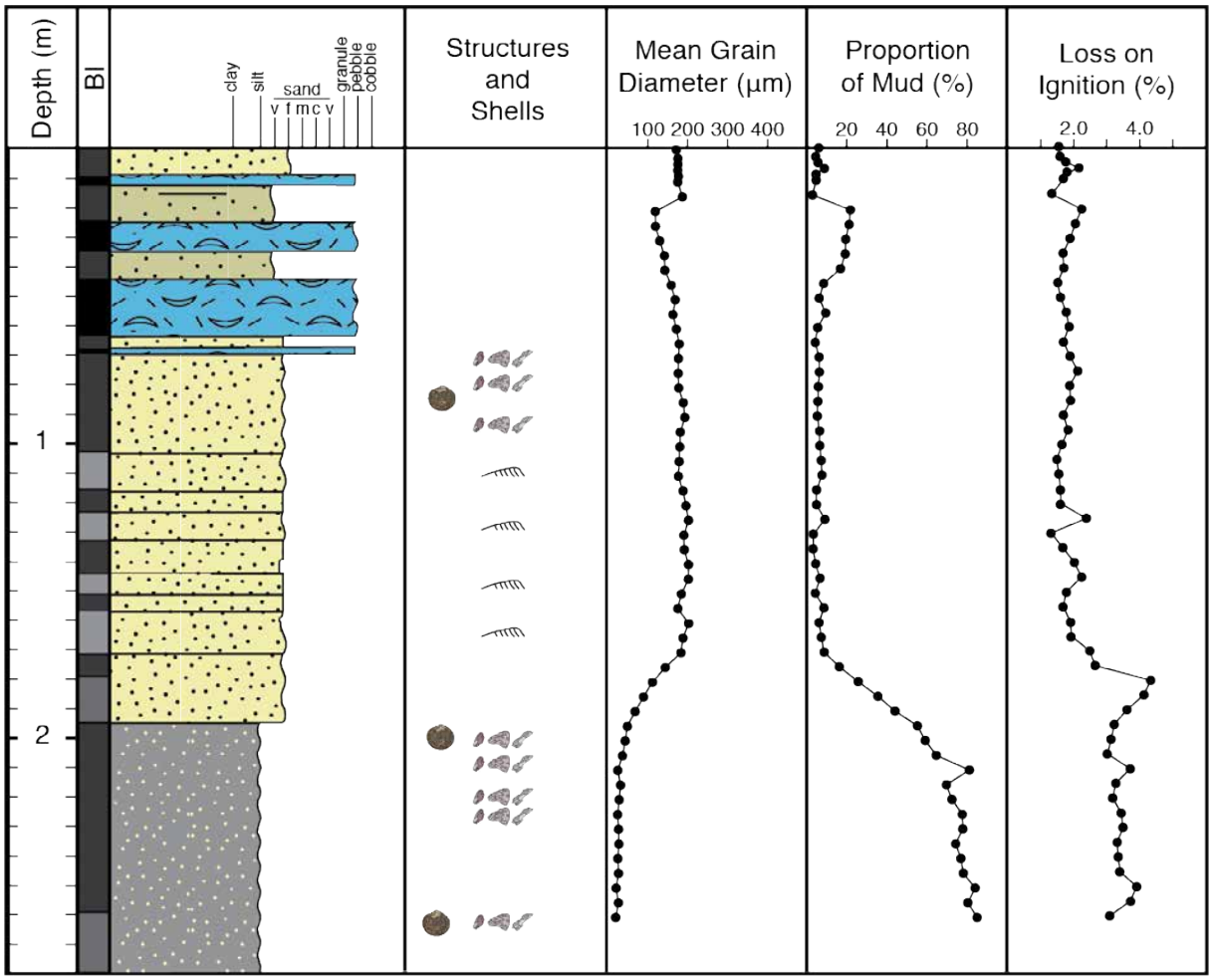
Depth (m)
BI
clay
silt
sand
v f m c v
granule
pebble
cobble
Structures and Shells
Mean Grain Diameter (µm)
100 200 300 400
Proportion of Mud (%)
20 40 60 80
Loss on Ignition (%)
2.0 4.0
1
2

Core G

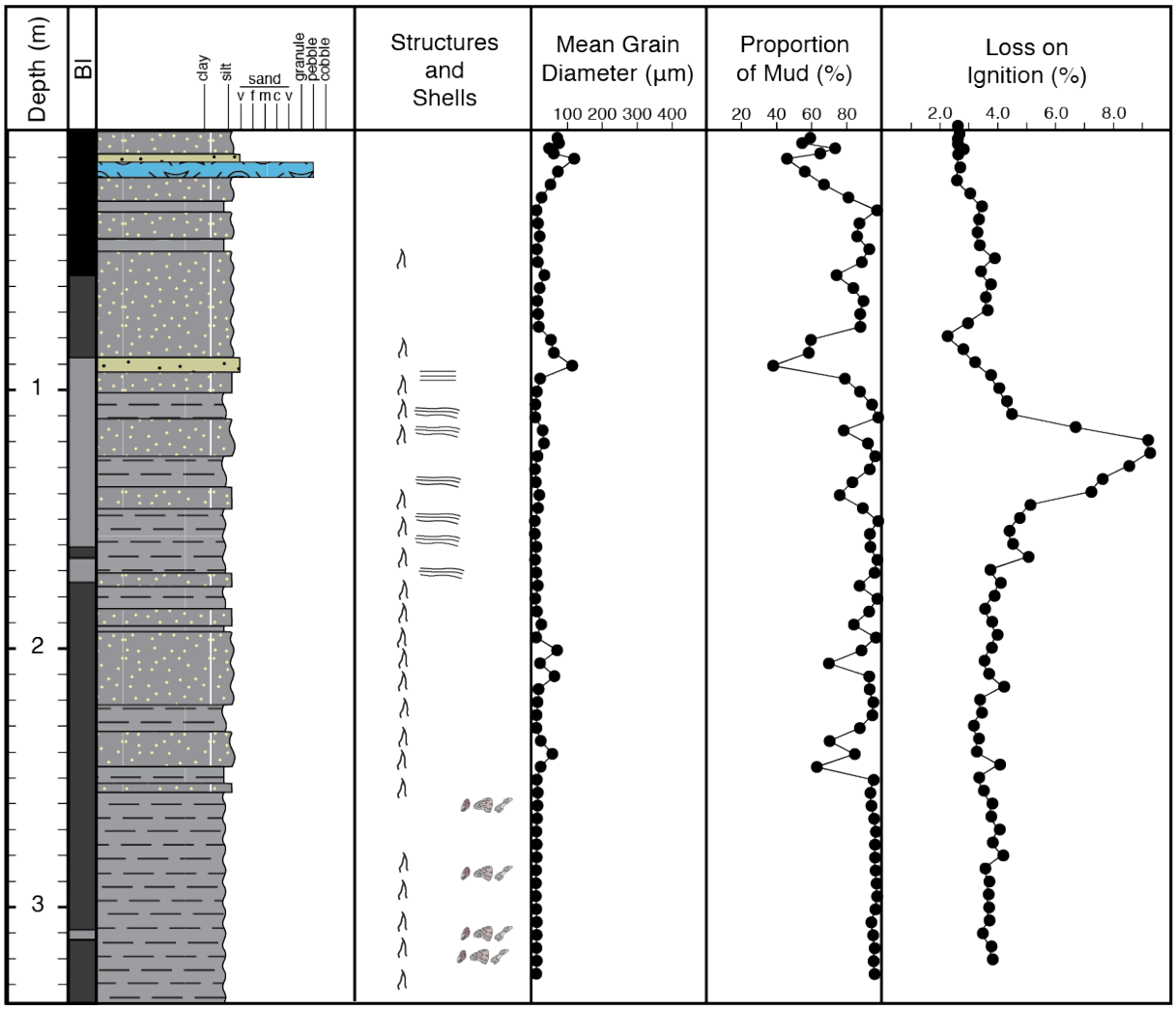
Depth (m)
BI
clay
silt
sand
v f m c v
granule
pebble
cobble
Structures and Shells
Mean Grain Diameter (µm)
100 200 300 400
Proportion of Mud (%)
20 40 60 80
Loss on Ignition (%)
2.0 4.0 6.0 8.0
1
2
3

Core H

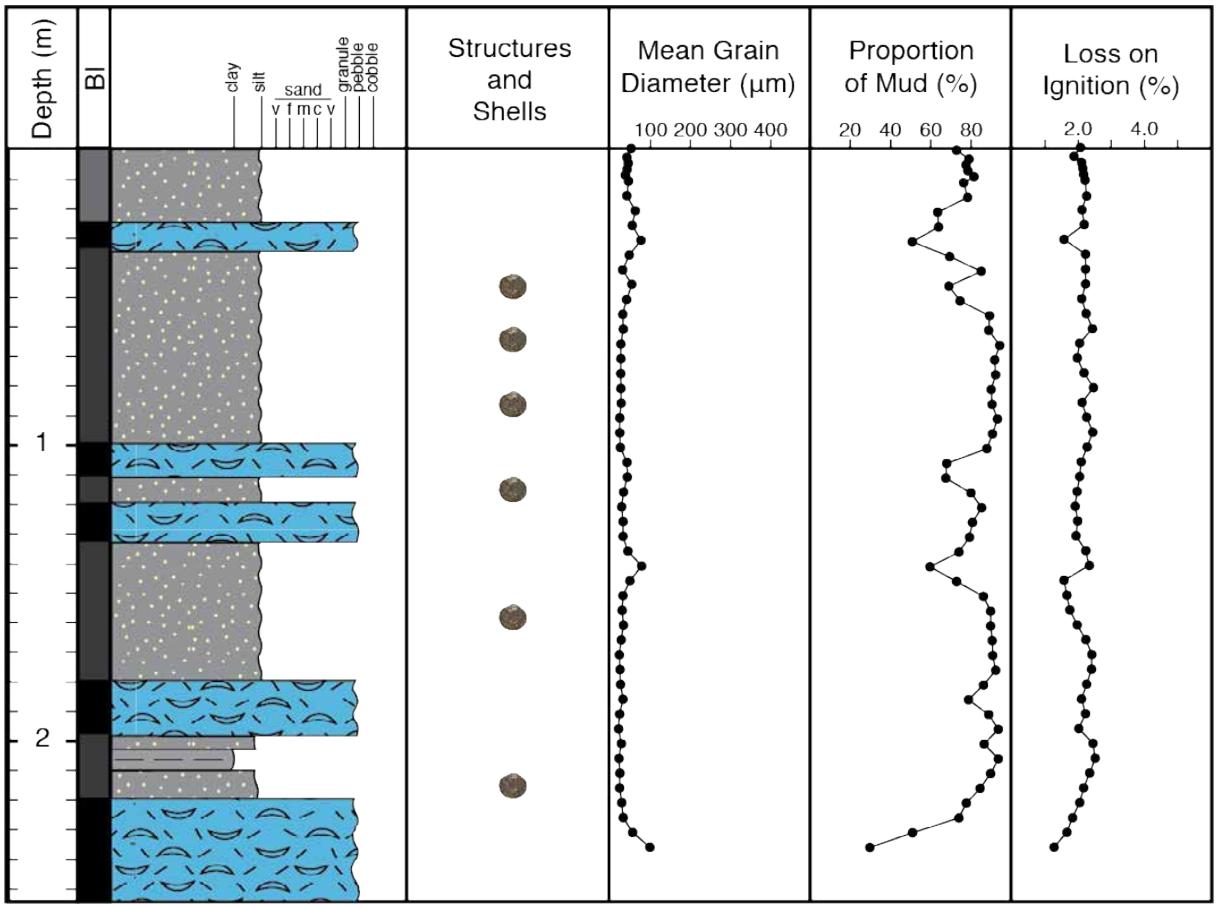
Depth (m)
BI
clay
silt
sand
v f m c v
granule
pebble
cobble
Structures and Shells
Mean Grain Diameter (µm)
100 200 300 400
Proportion of Mud (%)
20 40 60 80
Loss on Ignition (%)
2.0 4.0
1
2

Appendix D – X-radiographs of Boxcores

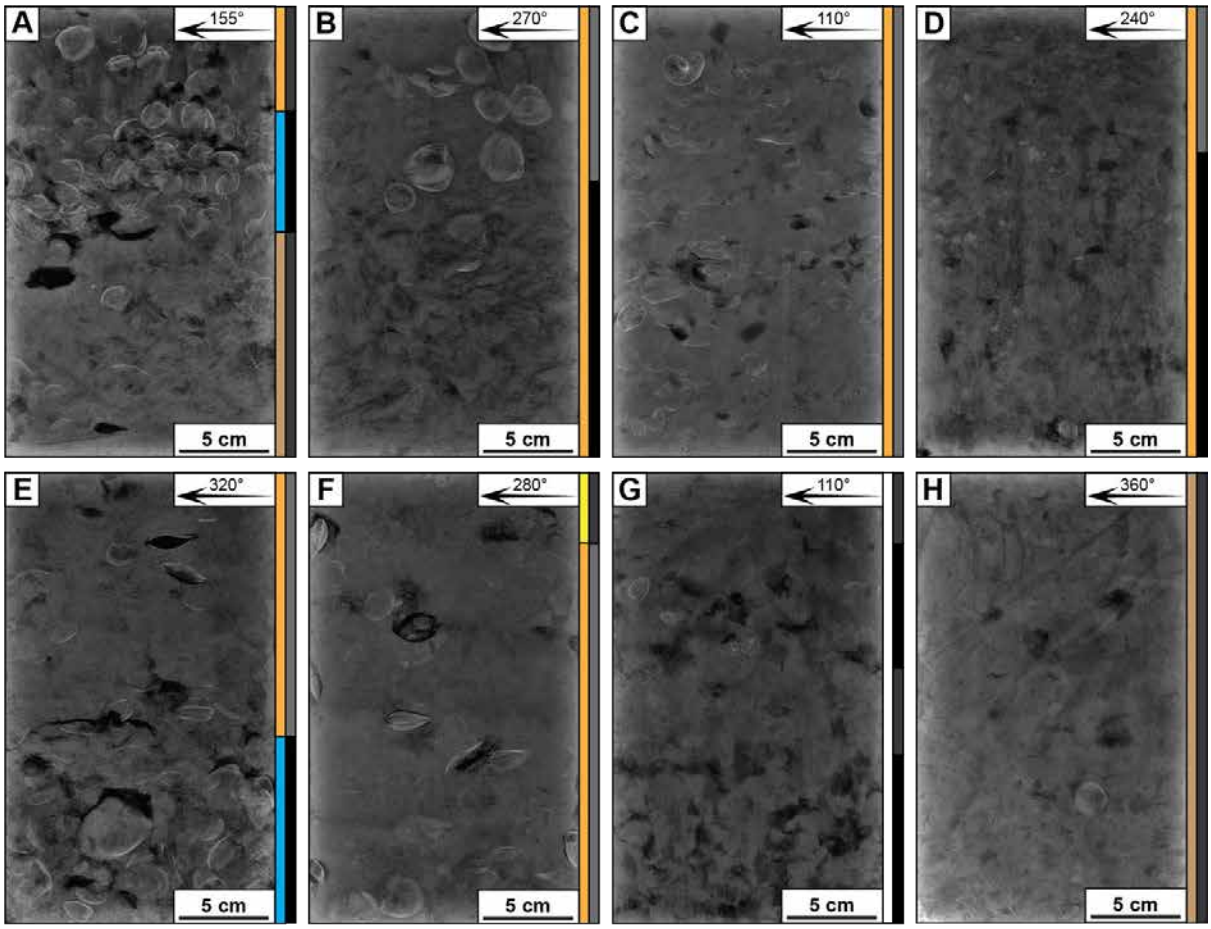

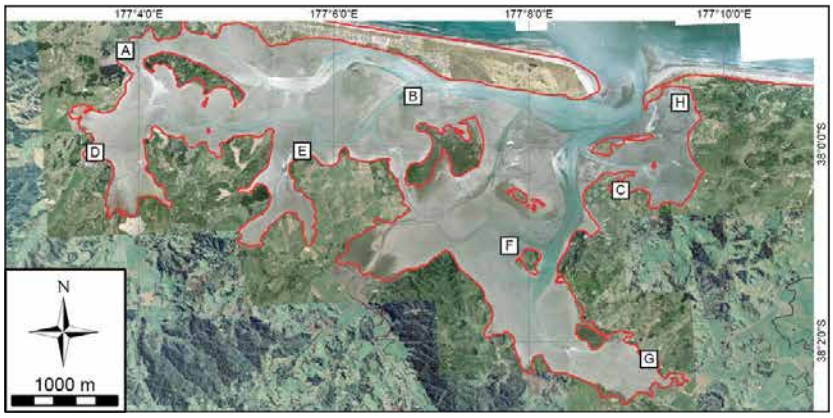

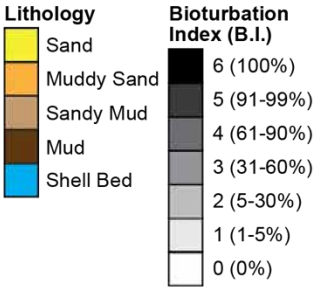

Appendix E – Grain Size Distribution Plots

Core Cumulative Proportion Plots

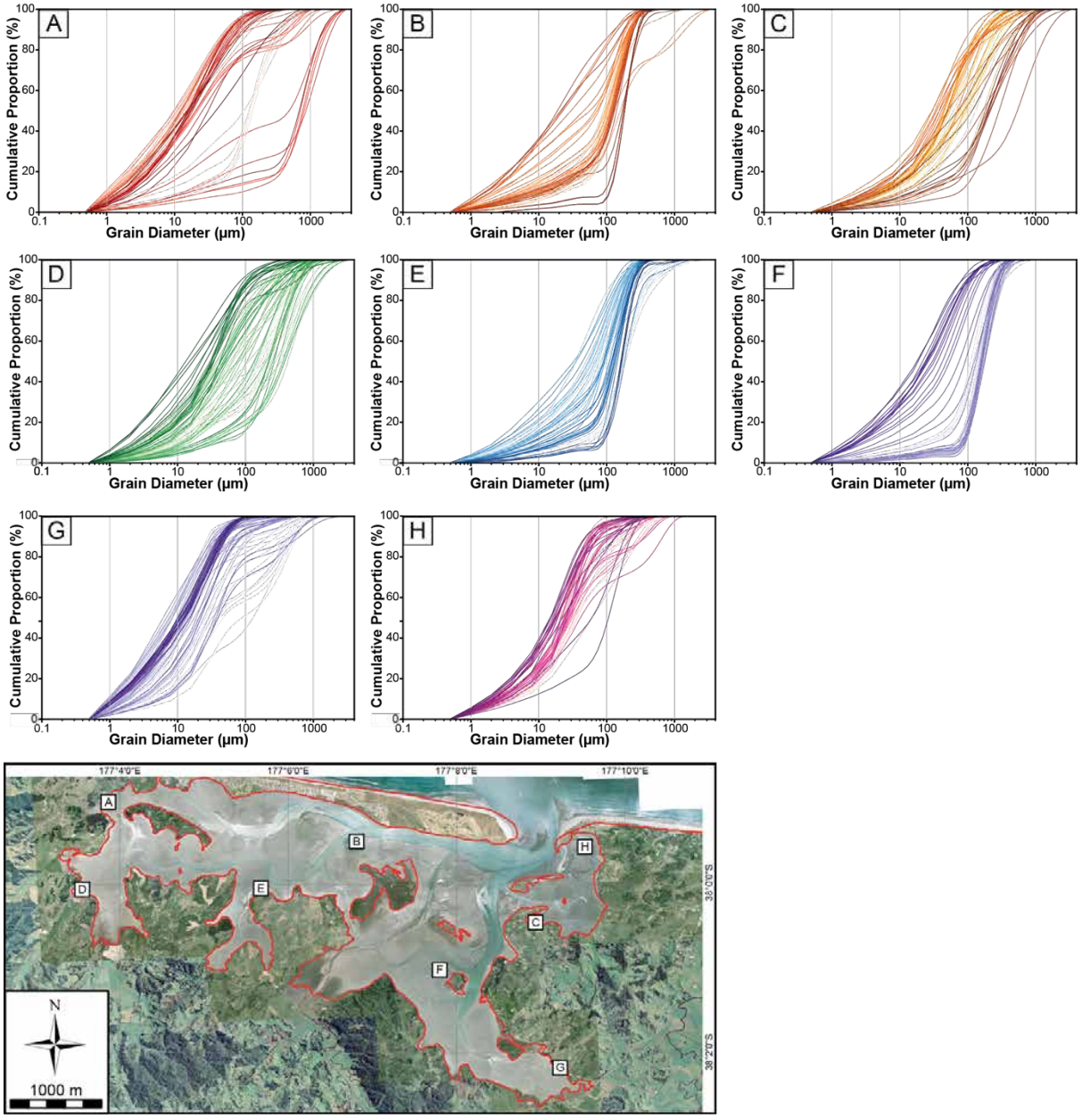

Core Frequency Distribution Plots

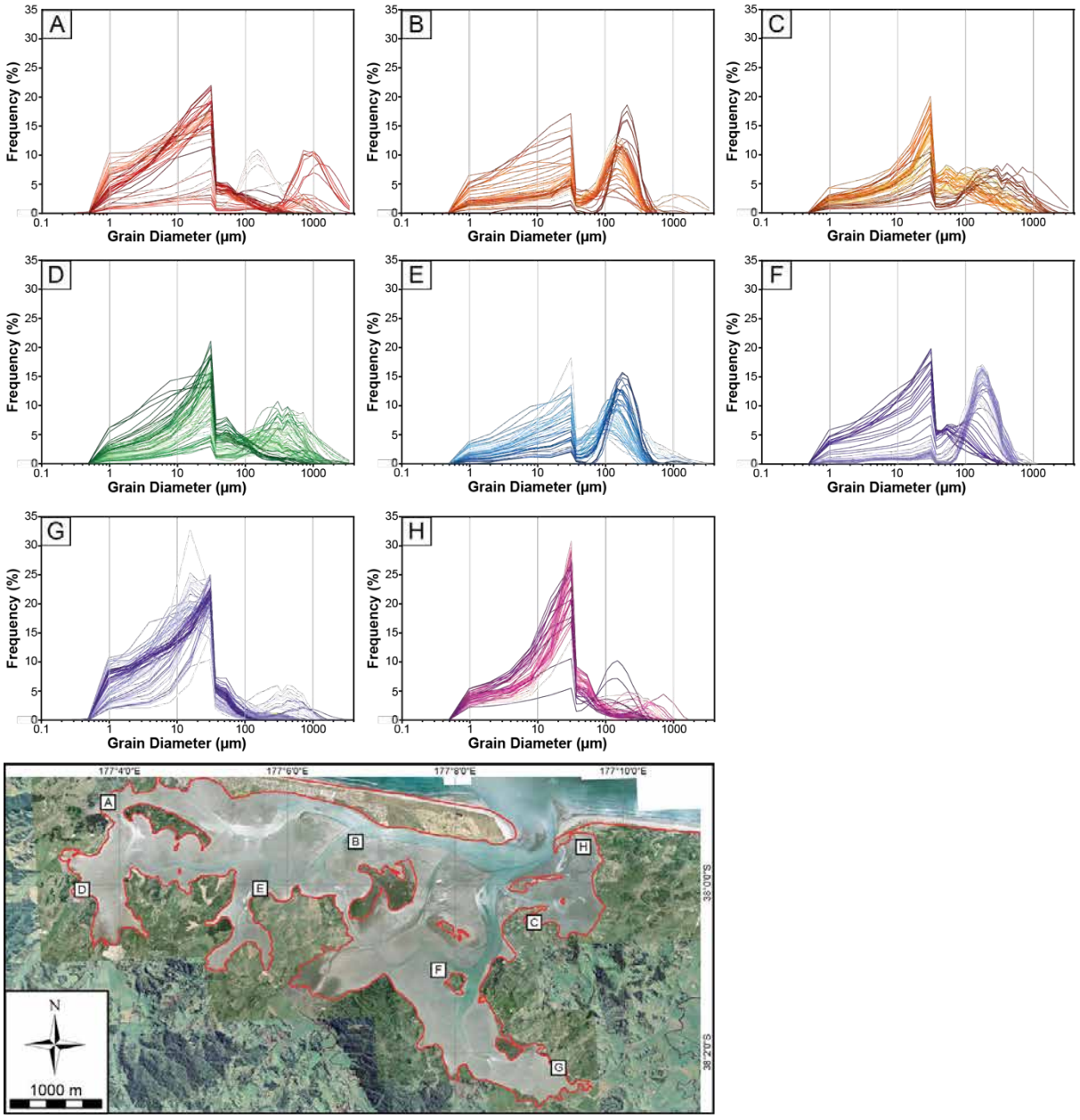

Surface Sediment Cumulative Proportion Plots

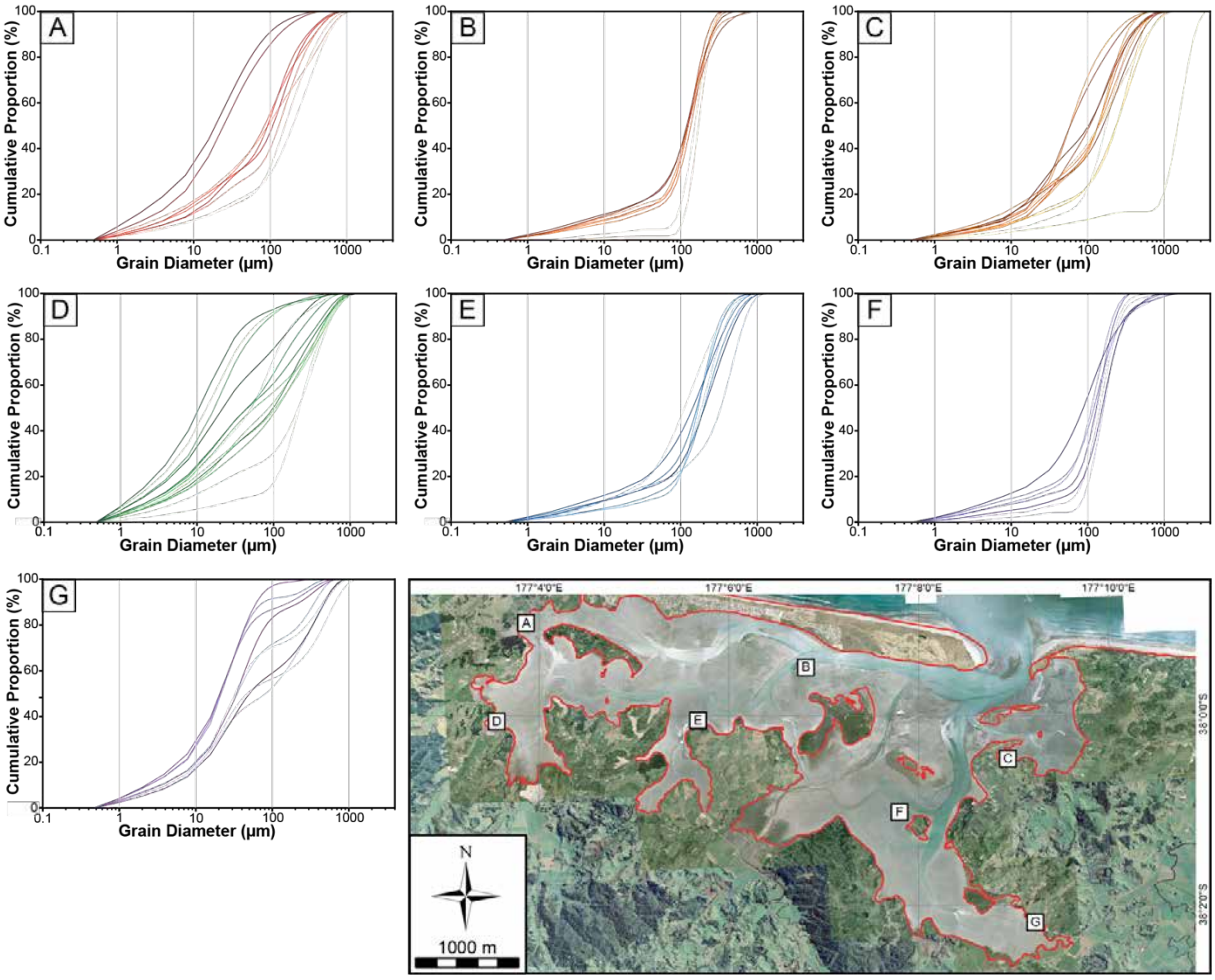

Surface Sediment Frequency Distribution Plots

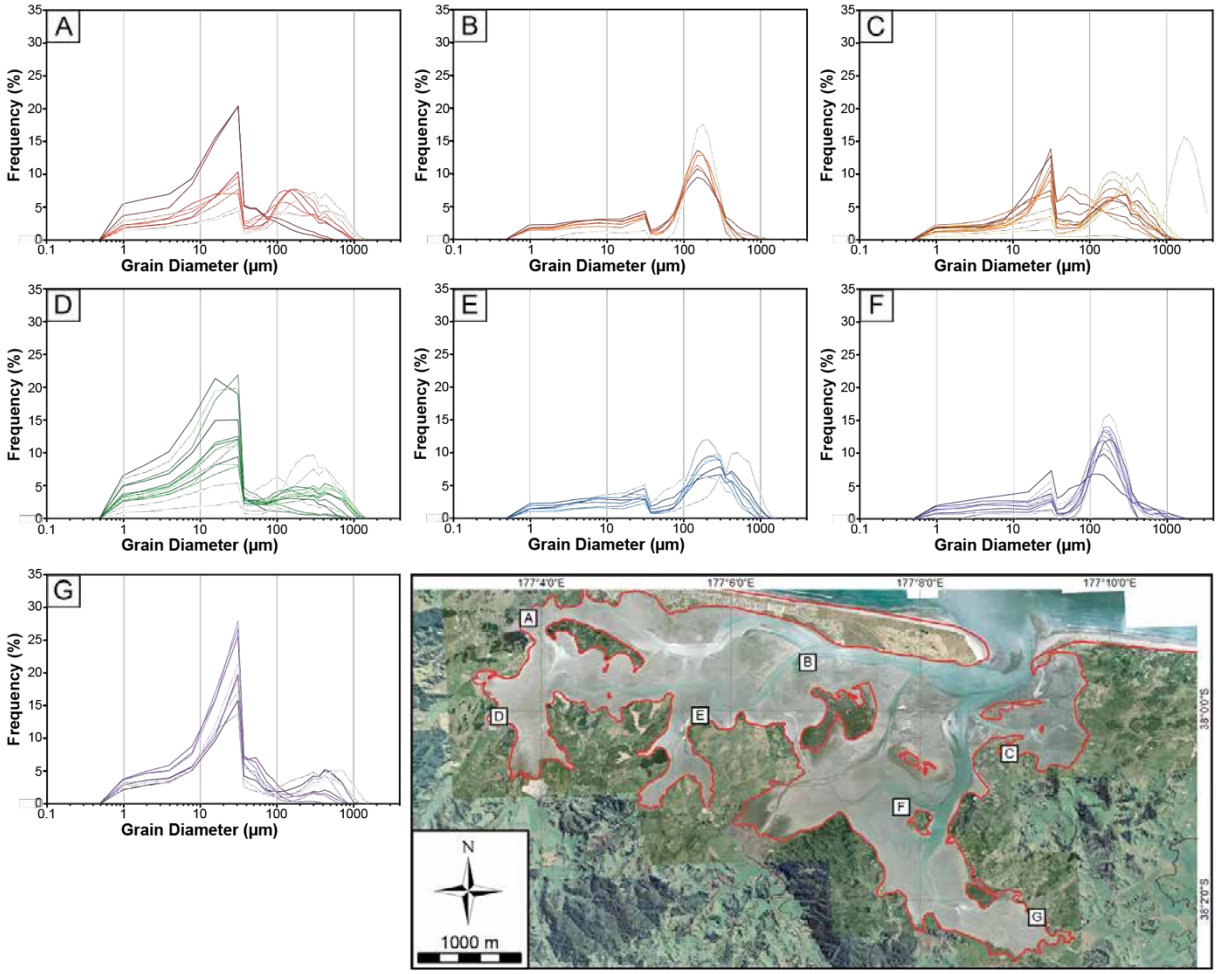

Appendix F – Grain Size and Loss on Ignition Maps

Mean Grain Size

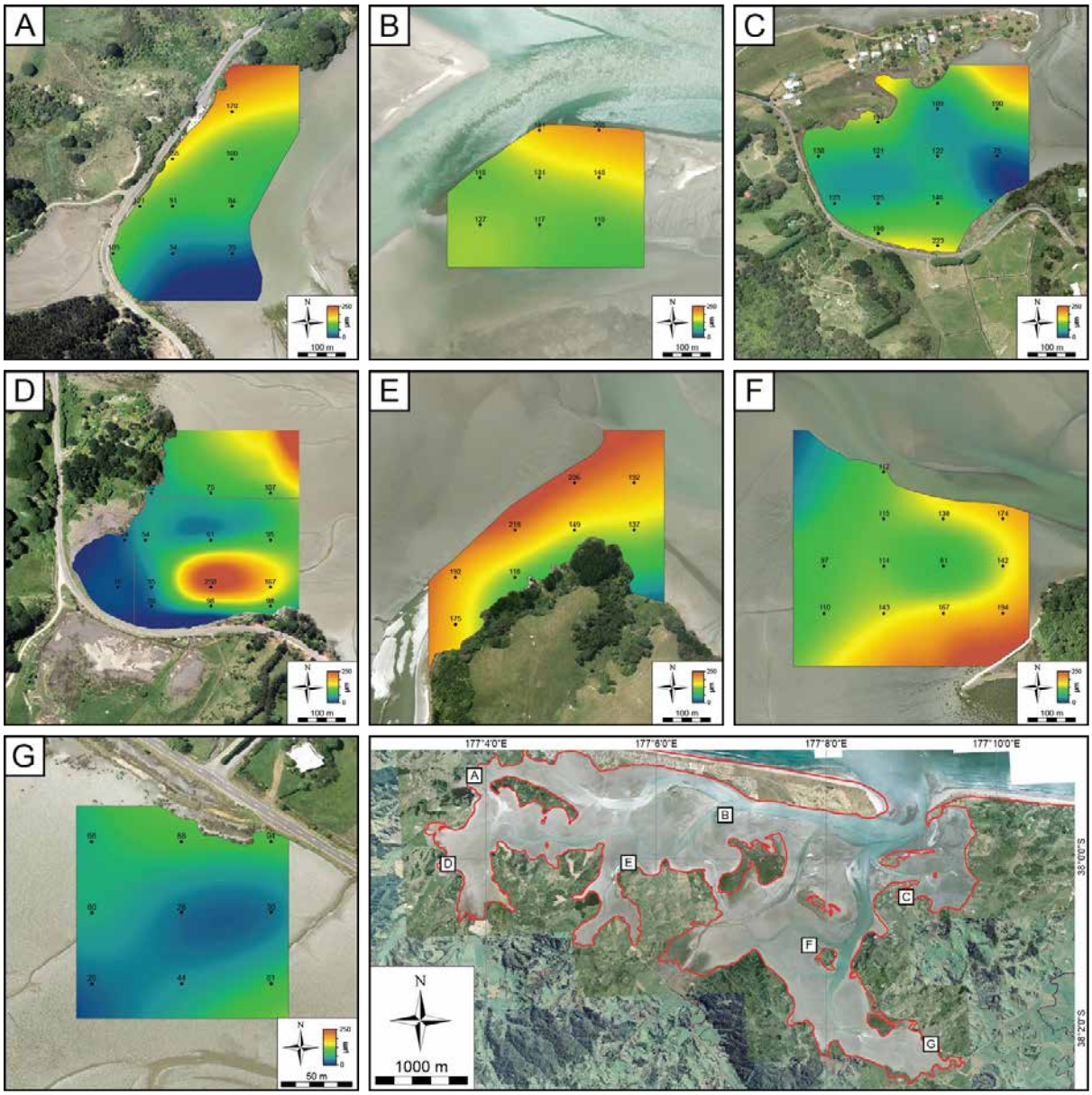

Proportion of Mud

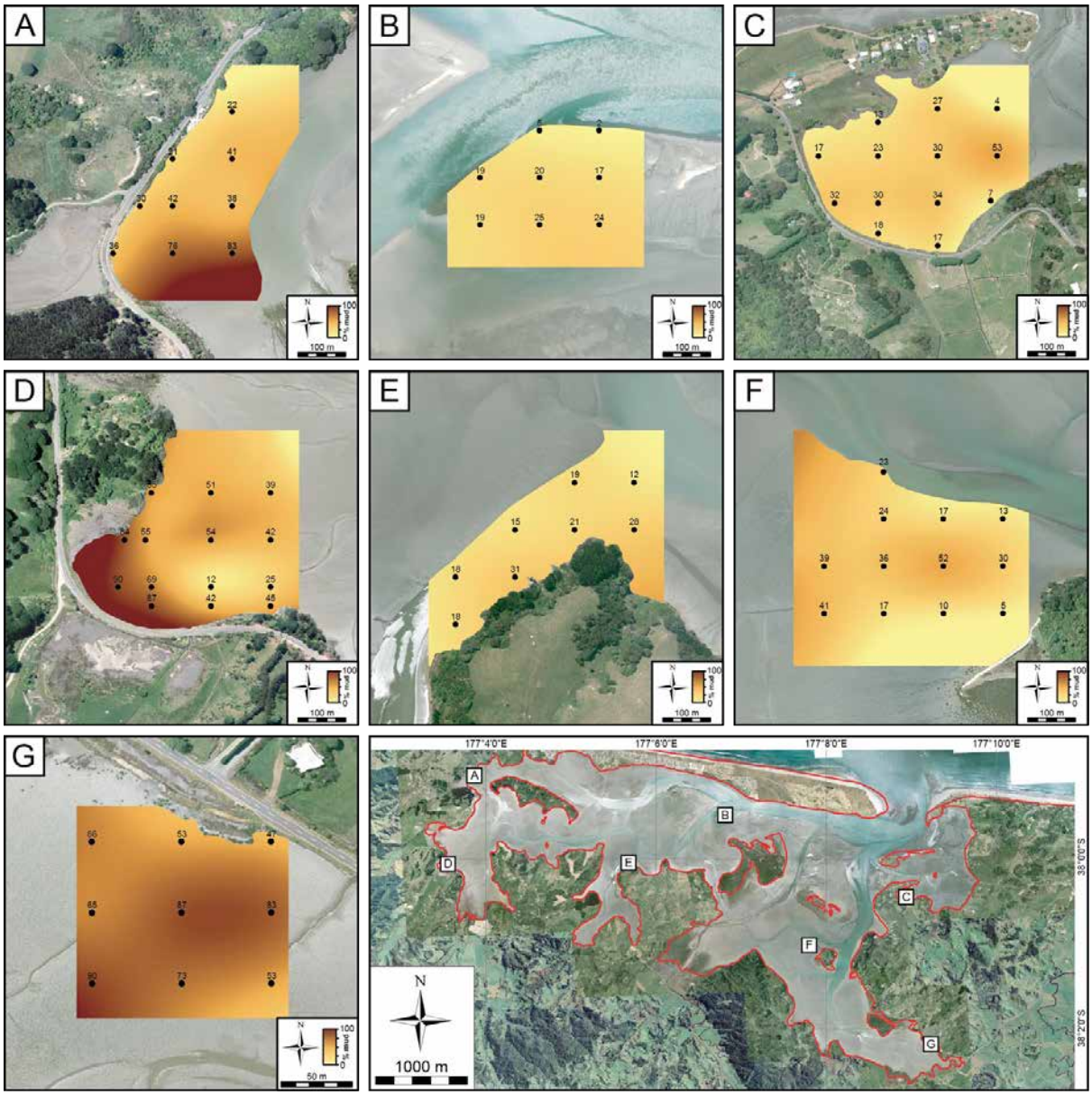

Loss on Ignition